EBioMedicine 58 (2020) 102895

Contents lists available at ScienceDirect

EBioMedicine

journal homepage: www.elsevier.com/locate/ebiom

Research paper

A surrogate of Roux-en-Y gastric bypass (the enterogastro anastomosis surgery) regulates multiple beta-cell pathways during resolution of diabetes in ob/ob mice

Chloé Amouyal[a,b], Julien Castel[c], Claudiane Guay[d], Amélie Lacombe[e], Jessica Denom[c], Stéphanie Migrenne-Li[c], Christine Rouault[a], Florian Marquet[a], Eleni Georgiadou[f], Theodoros Stylianides[g], Serge Luquet[c], Hervé Le Stunff[c], Raphael Scharfmann[h], Karine Clément[a,i], Guy A. Rutter[f,j], Olivier Taboureau[k], Christophe Magnan[c,1], Romano Regazzi[d,l,1], Fabrizio Andreelli[a,b,1,*]

[a] Sorbonne Université, INSERM, Nutrition and Obesities; Systemic approaches (NutriOmics), Paris, France
[b] AP-HP, Pitié-Salpêtrière Hospital, Diabetology department, F-75013 Paris, France
[c] Université de Paris, BFA, UMR 8251, CNRS, F-75013 Paris, France
[d] Department of Fundamental Neurosciences, University of Lausanne, Rue du Bugnon 9, CH-1005, Lausanne, Switzerland
[e] PreclinICAN, Institute of Cardiometabolism and Nutrition, Paris, France
[f] Section of Cell Biology and Functional Genomics, Division of Diabetes, Endocrinology and Metabolism, Department of Metabolism, Digestion and Reproduction, Imperial College London, London, UK
[g] Loughborough University, Loughborough, UK
[h] Université de Paris, Cochin Institute, Inserm U1016, Paris 75014, France
[i] APHP, Pitié-Salpêtrière Hospital, Nutrition department, F-75013 Paris, France
[j] Lee Kong Chian School of Medicine, Nan Yang Technological University, Singapore
[k] Université de Paris, BFA, Team CMPLI, Inserm U1133, CNRS UMR 8251, Paris, France.
[l] Department of Biomedical Sciences, University of Lausanne, Rue du Bugnon 7, CH-1005 Lausanne, Switzerland

ARTICLE INFO

Article History:
Received 4 May 2020
Revised 26 June 2020
Accepted 30 June 2020
Available online xxx

Keywords:
Diabetes
Bariatric surgery
Beta cell function
Insulin secretion
microRNA
ob/ob mouse

ABSTRACT

Background: Bariatric surgery is an effective treatment for type 2 diabetes. Early post-surgical enhancement of insulin secretion is key for diabetes remission. The full complement of mechanisms responsible for improved pancreatic beta cell functionality after bariatric surgery is still unclear. Our aim was to identify pathways, evident in the islet transcriptome, that characterize the adaptive response to bariatric surgery independently of body weight changes.

Methods: We performed entero-gastro-anastomosis (EGA) with pyloric ligature in leptin-deficient ob/ob mice as a surrogate of Roux-en-Y gastric bypass (RYGB) in humans. Multiple approaches such as determination of glucose tolerance, GLP-1 and insulin secretion, whole body insulin sensitivity, ex vivo glucose-stimulated insulin secretion (GSIS) and functional multicellular Ca^{2+}-imaging, profiling of mRNA and of miRNA expression were utilized to identify significant biological processes involved in pancreatic islet recovery.

Findings: EGA resolved diabetes, increased pancreatic insulin content and GSIS despite a persistent increase in fat mass, systemic and intra-islet inflammation, and lipotoxicity. Surgery differentially regulated 193 genes in the islet, most of which were involved in the regulation of glucose metabolism, insulin secretion, calcium signaling or beta cell viability, and these were normalized alongside changes in glucose metabolism, intracellular Ca^{2+} dynamics and the threshold for GSIS. Furthermore, 27 islet miRNAs were differentially regulated, four of them hubs in a miRNA-gene interaction network and four others part of a blood signature of diabetes resolution in *ob/ob* mice and in humans.

Interpretation: Taken together, our data highlight novel miRNA-gene interactions in the pancreatic islet during the resolution of diabetes after bariatric surgery that form part of a blood signature of diabetes reversal.

Funding: European Union's Horizon 2020 research and innovation programme via the Innovative Medicines Initiative 2 Joint Undertaking (RHAPSODY), INSERM, Société Francophone du Diabète, Institut Benjamin Delessert, Wellcome Trust Investigator Award (212625/Z/18/Z), MRC Programme grants (MR/R022259/1, MR/

* Corresponding author at: AP-HP, Pitié-Salpêtrière Hospital, Diabetology department, F-75013 Paris, France.
E-mail address: fabrizio.andreelli@aphp.fr (F. Andreelli).
[1] These authors contributed equally to this work.

https://doi.org/10.1016/j.ebiom.2020.102895

J0003042/1, MR/L020149/1), Diabetes UK (BDA/11/0004210, BDA/15/0005275, BDA 16/0005485) project grants, National Science Foundation (310030−188447), Fondation de l'Avenir.

Research in context

Evidence before this study

The restoration of beta cell functionality is an important challenge in the field of diabetology. Diabetes remission can be observed in humans in the days following bariatric surgery. The mechanisms of improvement of endocrine pancreas are still unclear. We validated in mice enterogastro-anastomosis with pyloric ligature (EGA) as a surrogate of Roux-en-Y gastric bypass (RYGBP) in humans, as a procedure that mimics all of the features observed after RYGBP, notably the rapid resolution of diabetes.

Added value of this study

In this study, we performed EGA in leptin-deficient *ob/ob* mice characterized by massive obesity, hyperglycemia and defective insulin secretion. We showed that, in this model, EGA enhanced glucose-dependent insulin secretion capacities in vitro and in vivo and normalized the glucose tolerance of ob-mice. Improvement of beta cell function was linked to changes, in pancreatic islet, of 193 genes expression and 227 biological processes, mainly involved in insulin secretion, glucose metabolism and ATP generation. We showed that 27 non-coding RNAs (miRNAs), known to be critical regulators of pancreatic beta cell physiology, were differentially regulated in the pancreatic islets by the surgery. Among them, 4 are central nodes of the miRNAs-genes interactions during the recovery of diabetes after bariatric surgery. Important role of these interactions was confirmed by the discovery that 4 miRNAs are part of a signature in blood specifically associated with diabetes remission not only in *ob/ob* mice but also in humans.

Implications of all the available evidence

Our data highlight complex miRNA-genes interactions during the resolution of diabetes after bariatric surgery and provide a molecular blood signature of diabetes resolution in mice and in humans.

1. Introduction

The restoration of normal pancreatic beta cell function and mass is an important challenge in diabetes research. Bariatric surgery approaches have been shown to promote restoration of physiological insulin secretion and to ameliorate insulin resistance during long-term follow-up [1,2]. However, surgery is invasive and can lead to complications. Better understanding of the mechanisms underlying the effects of bariatric surgery may, consequently, highlight new ways to elicit insulin secretion pharmacologically in diabetes.

Improvement of insulin secretion has been observed shortly after surgery, and independent of weight loss, using surgical procedures that have both restrictive and malabsorptive components (Roux-en-Y gastric bypass (RYGBP), duodenal switch or biliopancreatic diversion) and vertical sleeve gastrectomy [3–5]. Various mechanisms, including restoration of glucagon like peptide 1 (GLP-1) secretion, have been proposed to explain how surgery enhances insulin secretion and reduces hyperglycemia [6–9]. However, additional unknown mechanisms appear to be involved in the recovery of pancreatic beta-cell function post surgery since several studies evidenced improvement of glucose homeostasis after bariatric surgery independently of effective GLP-1 signaling pathway [10–12],

We have previously developed a model of bariatric surgery in mice and confirmed its capacity to cure diabetes in mice fed with a high fat diet [13]. In brief, this surgery is based on an entero-gastro-anastomosis (EGA) with pyloric ligature as a surrogate of Roux-en-Y gastric bypass (RYGB) in humans [13]. We demonstrated that EGA procedure recapitulate all features observed in humans after the RYGBP (reduction of food intake and of body weight, improvement of glucose homeostasis and of hepatic insulin sensitivity) as early as 10 days after surgery. Interestingly, in contrast to gastric lap-band, the EGA technique enhanced insulin secretion during an oral glucose challenge, and this effect contributed to the control of hyperglycemia. Circulating GLP-1 levels were modestly increased in the post-surgical period and the beneficial effects of EGA on insulin secretion were partly attenuated by continuous infusion of exendin [9−39] amide, suggesting that unknown additional factors contribute to beta cell recovery [13].

The mechanisms of post-surgical recovery of endocrine pancreas function are still unclear. From a clinical perspective, understanding the mechanisms of diabetes resolution is important to improving medical care after bariatric surgery. Indeed, post-surgical enhancement of beta cell functionality is not always observed. In some patients, it occurs independently of weight loss soon after bariatric surgery [5] and in others later, where it is more dependent on changes in weight [14]. Although it is critical to monitor the impact of diabetes therapy [15–17], post-surgical evaluation of endocrine pancreas function by measurement of classical parameters such as insulin or C-peptide can be difficult. The assessment of circulating biomarkers of beta cell function evolution may therefore be useful during post-surgical follow up and may help to adapt therapy and limit the occurrence of hypoglycemic or hyperglycemic events.

Here, we performed the EGA procedure in leptin-deficient ob/ob mice, a known model of diabetes and altered insulin secretion associated with massive obesity, inflammation and lipotoxicity. We showed that the EGA procedure fails to decrease hyperphagia permanently or to lower excess body weight. Nonetheless, glucose tolerance during oral glucose challenge was normalized after surgery when compared to lean C57BL6J wild type mice, and this effect was largely mediated by increased insulin secretion. Thus, we will take advantage of this model in which resolution of diabetes was observed independently of changes in diet and in body weight to identify new molecular pathways important for pancreatic beta cell recovery.

2. Methods

2.1. Lead contact and materials availability

Further information and requests for resources and reagents should be directed to and will be fulfilled by the Lead Contact, Chloé AMOUYAL (chloe.amouyal@aphp.fr). This study did not generate new unique reagents.

2.2. Experimental model and subject details

2.2.1. Animals and diet

Twelve-week-old male $lep^{-/-}$ ob-mice on a pure C57BL6J background (purchased from Janvier, Le Genest Saint Isle, France) were

acclimatized to our animal house under controlled temperature (22 °C) and light conditions (light/dark, 12 h/12 h) and were fed *ad libitum* with standard laboratory chow diet (no. 5058; Lab-Diet). All procedures were performed in accordance with the principles and guidelines established by the European Convention for the Protection of Laboratory Animals. The experimental protocol was approved by the ethics committee of Pierre and Marie Curie University under agreement number A 751,320.

2.2.2. Human cohort

Human blood analysis was performed on a subset of patients from our prospective cohort of bariatric surgery (Bariatric Surgery Cohort [BARICAN] $N = 2229$ patients with detailed phenotyping) from the Nutrition Department of Pitié-Salpêtrière Hospital (Paris, France) and the Institute of Cardiometabolism and Nutrition (Paris, France). Use of this cohort has ethical approval by CPP (P050318 Comites de Protection des Personnes [CPP] approval: 24 November 2006), CNIL (Commission nationale de l'informatique et des libertés; No. 1,222,666) and the French Ministry of Research. All patients provided informed consent. They are part of several studies registered on clinicaltrials.gov (NCT01655017, NCT01454232). Diabetes remission refers to the American Diabetes Association (ADA) definition [18]. This definition was used to define 1-year remission outcomes[19] (i.e. diabetes remission (DR....): HbA1c <6.0%, fasting plasma glucose <5.6 mmol/l without any use of glucose-lowering agents at 1-year and non diabetes remission (NDR): HbA1c>6.5%, fasting plasma glucose >7.0 mmol/l or the use of glucose-lowering agents at 1-year).

2.3. Method details

2.3.1. Surgical procedure

The EGA procedure was performed as previously described [13]. In brief, *ob/ob* mice undergoing surgery were fasted for 6 h and anaesthetized with 2% isoflurane (Abbott, Rungis, France) and air/oxygen. Analgesia was delivered intraperitoneally 30 min. before surgery (Buprenorphine, 0.03 mg/kg, Axience SAS, France) and at the end of the procedure (Ketoprofen, Merial, 1%, diluted 1/100, 200 μL per mouse). Antibioprophylaxy was delivered sub-cutaneously at beginning of the surgery (ceftriaxone 100 mg/kg, Hospira, USA). The procedure consisted of a pyloric sphincter ligature, followed by an entero-gastric anastomosis allowing the exclusion of the duodenum and the proximal jejunum of the alimentary tract. Sham-operated mice (simple laparotomy) underwent the same duration of anaesthesia as EGA mice. In both groups, the laparotomy was repaired in two layers. All mice were maintained on a standardized post-operative protocol to monitor pain, body weight and hydration, subcutaneous injection of saline serum and additional analgesia was given as necessary. The mice had access to water and mixed chow diet right after surgery. Post-surgical survival rates were 50% in EGA-ob mice and 80% in sham-ob mice.

2.3.2. Study design

Twelve-week-old *ob/ob* mice were randomized to EGA or sham surgery. Animals were followed up for one month and then sacrificed. A sham-ob mouse group was pair-fed to the EGA-ob mouse group following surgery for eight days. After this period, both groups were provided chow diet *ad libitum*. Blood was collected once a week from the tail vein to determine random fed glucose levels with a glucometer (Accuchek performa®, Roche). Body weight and food intake were monitored daily in the morning during the follow-up in the first 15 EGA-ob mice and 15 sham-ob mice. Body composition, glucose tolerance and insulin sensitivity were assessed one week before the surgery and at the end of the follow-up. There is no definition of diabetes remission or resolution for rodent model. We therefore chose to compare AUC of glycemia during OGTT with those of C57Bl6J mice (+/- 10%). Similar or lower values of AUC was our definition of normo-glucose tolerance and therefore diabetes remission after surgeries. Blood was collected before the surgery and at the sacrifice for the assessment of biochemical and hormonal parameters. Specific groups of EGA and sham-ob mice were dedicated to the study in metabolic chambers (energy expenditure, locomotor activity and food intake monitoring (Labmaster; TSE Systems, Bad Homburg, Germany), intraperitoneal treatment with exendin [9-39] amide.

2.3.3. Exendin [9−39] amide and leptin administration

For exendin [9−39] amide infusion experiments, the intraperitoneal cavity of EGA-ob mice was continuously infused for 28 days with exendin [9−39] amide (Sigma Aldrich®, ref E7269) at the rate of 2 pmol. $kg^{-1}.min^{-1}$ ($6{,}74^{-06}$ mg. $kg^{-1}.min^{-1}$) or NaCl (0.9%) with an osmotic minipump (Alzet Model 2004; Alza, Palo Alto, CA). At this rate of infusion, GLP-1 receptor signaling is blocked selectively and without off target effects [20,21]. Exendin [9−39] amide and saline infusions by Alzet pump were started during the EGA procedure. In another experiment, Ob-mice were injected once a day, intraperitoneally, with leptin (Sigma Aldrich®, ref L3772) at the rate of 640 μg/day (equivalent to 12.8 mg.kg^{-1}.day for a 50 g mouse) or 0.9% NaCl (0.9%) during 14 days.

2.3.4. Body composition

Body composition was measured in unanesthetized mice using the Bruker Minispec mq10 NMR (Bruker Optics, Billerica, MA) one week before the surgery and at day 28 after the surgery. Animals were placed in a clear plastic cylinder (50 mm in diameter) lowered into the device for the duration of the scan (<2 min). Body composition was expressed as a percentage of body weight.

2.3.5. Metabolic measurements

Blood was withdrawn from the tail vein for both fed and fasted experiments using EDTA as the anticoagulant. Blood glucose levels were evaluated using a glucometer (Accuchek performa®, Roche). Serum insulin was measured by Elisa (Alpco, Eurobio). For active GLP-1 determination, blood was collected into EDTA coated Microvettes (SARSTEDT) preloaded with enzyme inhibitor cocktail (p2714 Sigma-Aldrich) and Dipeptidyl peptidase-4 inhibitor (Merck, Millipore, USA). Peripheral plasma active GLP-1 was measured during oral glucose tolerance test (OGTT). Blood was immediately centrifuged at 4 °C to separate the plasma from the whole blood and stored at −20 °C until analysis. Serum glucagon, c-peptide, PYY, pancreatic polypeptide, active GLP-1, GIP, total adiponectin, TNF-a, IL-6, MCP-1 and resistin concentrations were assessed by MILLIPLEX assays (MMHMAG-44 K Milliplex, EMD Millipore, St. Charles, MO, USA). Serum concentrations of triglycerides, free fatty acids (FFAs), ketone bodies, and glycerol were determined using an automated Monarch device (CEFI, IFR02, Paris, France) as described previously [22].

2.3.6. Glucose and insulin tolerance tests

A glucose tolerance test (1.5 g/kg body weight) was performed on mice fasted overnight for 14−16 h. Blood glucose levels were determined at 0, 15, 30, 60, and 90 min. For the insulin tolerance test, animals fasted for 5 hr were injected intraperitoneally with 0.75 or 2 units of insulin/kg body weight (Novorapid®, Novo-Nordisk, La Défense, France), and glucose levels were measured 0, 15, 30, 60 and 90 min post-injection.

2.3.7. Measurement of food intake and energy expenditure

Mice were monitored for energy expenditure, oxygen consumption and carbon dioxide production, respiratory exchanged rate (RER; $V{\cdot}CO_2/V{\cdot}O_2$), food intake and spontaneous locomotor activity using metabolic cages (PhenoMaster/LabMaster, TSE Systems). Mice were individually housed and acclimated to the chambers for 48 h before experimental measurements. In the chambers, food and water consumption was measured automatically. All food intake is reported

in kilocalories per day or kilocalories per 12-h dark or light period. Locomotor activity was recorded using infrared light beam-based locomotion monitoring system (beam breaks/h). Data analysis was carried out with Excel XP (Microsoft France, Issy-Les-Moulineaux, France) using extracted raw values of $V{\cdot}O_2$, $V{\cdot}CO_2$ (in ml/h) and energy expenditure (kJ/h). Subsequently, each value was expressed either per total body weight or whole lean tissue mass extracted from the Bruker Minispec mq10 NMR analysis.

2.3.8. Histological analysis of pancreas

Immunohistochemistry was performed on 7 μm sections of paraffin-embedded pancreatic tissue. With a random start between the first 50 sections, every 50th section was sampled. 10 sections, separated by 50 sections, were stained for insulin by incubation with a primary guinea pig anti-porcine insulin antibody (dilution 1:50; Bio Rad, 5330−0104 G, RRID: AB_1,605,150), followed by incubation with polyclonal rabbit anti guinea pig immunoglobulins marked with peroxydase (dilution 1:50; Dako, Glostrup Denmark, ref P0141) and subsequently visualized by diaminobenzidine (DAB, kit DAB SK-4100 Vector-Biosys, SK-4100, RRID: AB_2,336,382) and counterstained by hematoxylin.

Insulin-stained sections were used for morphometric analysis. Quantitative evaluation was performed using the Histolab 6.0.5 software (Microvision Instruments, Evry, France). Insulin positive area/mm2 of pancreas was calculated by dividing the insulin positive area by the total pancreas surface of each analyzed section.

Immunochemistry with immunofluorescent antibodies. We used the following primary antibodies: anti-mouse insulin (1/2000, Sigma, Cat# I2018, RRID: AB_260,137) and secondary antibodies anti-mouse Alexa Fluor 594 antibodies (1/400, Jackson ImmunoResearch Labs Cat# 115−585−003, RRID: AB_2,338,871). We stained the cell nuclei with the Hoechst 33,342 fluorescent stain (0.3 mg/ml, Invitrogen, France).

2.3.9. Islet isolation and ex vivo *glucose-stimulated insulin secretion*

At sacrifice, the whole pancreas was digested with collagenase (collagenase P, Sigma Aldrich, France) injected through the pancreatic duct. Pancreases were incubated at 37 °C for 10 min. to complete digestion. After several wash by cold buffer containing (HBSS: Gibco, Invitrogen, France; BSA, Interchim SA, BSA and Hepes: Gibco, Invitrogen, France); islets were separated using a Histopaque 1119 (Sigma Aldrich, France) and HBSS gradient and picked up manually.

After isolation, islets were incubated for 20 h in a RPMI media containing (RPMI medium 1640: Gibco, Invitrogen, France; 10% inactivated fetal calf serum (FCS), 1% Hepes, 11 mmol/l glucose (D-Glucose 45%, Sigma Aldrich, France), 100 IU/ml penicillin, and 100 μg/ml streptomycin). To attend insulin secretion capacities, islets were placed in a 24-well plate to be treated in the presence of different glucose concentration.

2.3.10. Flow cytometry analysis

Cells released by the digestion of islets with trypsin were resuspended in PBS containing 1% BSA and 2 mM EDTA. For mouse cells, we used anti-CD45-APC-eF780 (30F11) from Biolegend (Cat# 103,111, RRID: AB_312,976), anti-insulin-A647 (C27C9) from Cell Signaling Technology (Cat# 9008, RRID: AB_2,687,822), anti-glucagon-BV421 (U16−850) from BD biosciences (Cat# 565,891, RRID: AB_2,739,385), anti-ki67-PE (REA 183) (Cat# 130−100−289, RRID: AB_2,652,551) and Viobility 405/520 Fixable dye from Miltenyi Biotec. For intracellular staining, we used Foxp3 Transcription Factor Staining Buffer Set from ebioscience. FACS analysis was performed with an LSRFortessa Analyzer (BD Biosciences).

2.3.11. Measurement of intracellular free calcium

Functional multicellular Ca^{2+}-imaging was performed on isolated islets. Islets were incubated with Cal-520 (Stratech) for 45 min. at 37 °C in KREBS-Ringer buffer (KBH: 140 mM NaCl, 3.6 mM KCl, 0.5 mM NaH_2PO_4, 2 mM $NaHCO_3$, 1.5 mM $CaCl_2$, 0.5 mM $MgSO_4$, 10 mM HEPES) supplemented with 3 mM glucose. Fluorescence imaging was performed on a Zeiss Axiovert confocal microscope using a Nipkow spinning disk head, and 10 × −20 × /0.3−0.5 NA, EC Plan-Neofluar objective (Zeiss) allowing rapid scanning of islet areas for long periods of time with minimal phototoxicity. Velocity software (PerkinElmer Life Sciences) provided the interface while islets were kept at 37 °C and constantly perifused with KHB containing 3 or 17 mM glucose or 20 mM KCl. For each experiment, 21−31 islets were used. Imaging data were analysed with ImageJ software using an in-house macro, available upon request.

2.3.12. miRNA and mRNA expression profiling (microarray)

Total RNA was extracted from pancreatic islets using the miRNeasy micro kit (Qiagen). Global miRNA expression profiling was carried out at the Genomic Technologies Facility of the University of Lausanne using miRNA gene microarrays (Agilent Technologies, Morges, Switzerland). Data were submitted to GEO repository. Changes of interest were confirmed by qPCR. In brief, mature miRNA levels were measured using the miRNACURY LNA™ Universal RT followed by miRNA PCR kit (Exiqon). Results were normalized by mmulet-7f-5p, as determined by the NormFinder test[23].

Profiling of mRNA was performed by Arraystar (MD, USA) using Agilent Technologies and Agilent GeneSpring GX v12.1 software for data analysis. The sample preparation and microarray hybridization were performed based on the manufacturer's standard protocols. Briefly, total RNA from each sample was amplified and transcribed into fluorescent cRNA with using the manufacturer's Agilent's Quick Amp Labeling protocol (version 5.7, Agilent Technologies). The labeled cRNAs were hybridized onto the Whole Mouse Genome Oligo Microarray (4 × 44 K, Agilent Technologies). After having washed the slides, the arrays were scanned by the Agilent Scanner G2505C. Data were submitted to GEO repository.

2.3.13. Quantitative RT-PCR

Total RNA was extracted from pancreatic islets using the miRNeasy micro kit (Qiagen). Reverse transcription was performed using Superscript IV and random hexamer (Promega). We performed a Quantitative PCR with SybrGreen and normalized each transcript by 18S, beta actin and cyclin A expression to obtain relative quantification. Upon request, all primers can be provided.

2.4. Quantification and statistical analysis

*2.4.1. Pearson (*R*)-based connectivity and correlation analyses*

Correlation analyses between the Ca^{2+} signal time series for all cell pairs in an imaged islet were performed in MATLAB using a custom-made script [24]. A noise reduction function (effectively a rolling average) was applied to smooth noisy data and minimize the effects of outliers. The data window size used to calculate the moving averages was set to 5% of the total data points collected during capture at each condition (3 mM glucose: every 6 data points, 17 mM glucose: 24 points, KCl: 8 points). Results were not affected when these rolling averages covered more points (less smoothing) i.e. over 10%, 15% and 20% of the points analysed under each condition (not shown). All traces were normalised to minimum (basal) fluorescence (F_{min}). The correlation function R between all possible (smoothed) cell pair combinations (excluding the autocorrelation) was assessed using Pearson's correlation. Data are displayed as heatmap matrices, indicating individual cell pair connections on each axes (min. = 0; max. = 1). The Cartesian co-ordinates of the imaged cells were then taken into account in the construction of connectivity line maps. Cell pairs were connected with a straight line, the color of which represented the correlation strength and was assigned to a color-coded light-dark ramp (R = 0.1−0.25 [blue], 0.26−0.5 [green], R = 0.51−0.75 [yellow],

$R = 0.76-1.0$ [red]). The positive R values (excluding the auto-correlated cells) and the percentage of cells that were significantly connected to one another were averaged and compared between groups.

2.4.2. Statistical analysis

Data are expressed as means ± SEM. Statistical significance was assessed using Student's *t*-test and 1-way ANOVA or Mann and Whitney test and Kruskal Wallis for non-parametric analysis to examine the effect of multiple variables. Two-way ANOVA was performed in the study of glucose and insulin tolerance P-values <0.05 were considered significant. Statistical analysis was performed with GraphPad Prism (GraphPad Software version 7.0).

Multidimensional scaling (MDS): A multidimensional scaling analysis was performed using the gene expression vectors, represented by each sample for dimension reduction and representation of the sample's distribution.

Differential expressed genes analysis (DEG): Three differentially expressed genes (DEG) analysis was performed i.e. EGA ob-mice vs C57BL6J (WT), Sham ob-mice vs WT and EGA ob-mice vs sham ob-mice using edgeR package[25] in Bioconductor. The gene expressions of the 12 samples were normalized using the TMM method for normalization of sequencing data and a Fisher's Exact Test with common dispersion was applied to determine differential expression. P value and False discovery rate (FDR) were reported by edgeR. Genes with a FDR adjusted p value ≤ 0.001 and, a log fold change (logFC) ≤ -1 and ≥ 1 were conserved. Results of down and up -regulated genes for the three DEGs analysis are depicted on Venn diagrams and volcano plot. The figure was obtained using the ggplot2 R package [26].

Enrichment analysis: Pathways and GO terms enrichment analysis were performed using the "Clusterprofiler" package in R[27] in order to search shared biological functions among genes highly deregulated. The most significant genes deregulated in each DEG analysis were used and mapped to GO terms, Gene ontology Term [28] in order to identify significant biological processes, molecular functions and cellular components deregulated. P values and p adjusted values allowed to rank of GO terms from the most to the less significant (classified by enrichment adjusted p-value or by gene ratio). miRNA-genes network: To assess potential miRNA effect within target mRNAs from our studies, the targetScanMouse tool (http://www.targetscan.org/mmu_72/) was used [29]. Basically, all the genes predicted for the 27 selected miRNAs by the targetScanMouse were downloaded. Then, a biological network was built if one of the 193 genes were annotated to one of the 27 selected miRNAs. The network was built using Cytoscape (version 3.7) [30].

2.5. Data and code availability

The data from islets' mRNA and miRNA profiling (microarrays) generated during this study are available at GEO repository number GSE133852.

3. Results

3.1. EGA procedure does not modify food intake, energy expenditure or body weight

In our previous report [13], the EGA procedure was shown to reduce food intake and body weight strongly in high fat diet-fed mice. In marked contrast, in the *ob/ob* model used here, we found the decrease of both parameters in EGA ob-mice was transient and comparable to sham group pair-fed mice during the 10 days following surgery (Fig. 1a-b, suppl Fig. 1a). After this period, food intake and body weight started to recover. At the end of the follow-up period (28 days) these parameters reached the level observed before surgery (Fig. 1a-b, suppl Fig. 1a), with a similar evolution up to 80 days after surgery (Fig. 1b). Consequently, most of the biochemical blood parameters (triglycerides, free fatty acids, glycerol, beta hydroxy-butyrate) measured at the beginning and at the end of the follow-up period were similar in EGA-ob mice and sham-ob mice (Table S1).

The above biphasic evolution might be linked to post-operative stress in this particular model [31]. Because the maintenance of a similar body weight does not exclude changes in fat and lean mass, we studied body composition before and 30 days after surgery. At both time points, fat and lean mass were not different between EGA-ob mice and sham-operated animals (suppl Fig. 1b). Additionally, a lack of changes in body fat distribution was confirmed by measuring similar fat pad depots in both groups (data not shown). *Ob/ob* mice are a well-known genetic model of deficiency in the anorexigenic hormone, leptin. However, monitoring of daily food intake demonstrated that the EGA procedure was not sufficient to reduce food intake in *ob/ob* mice, suggesting that leptin is probably an important mediator of the satietogenic effect of EGA surgery in wild-type mice (Fig. 1a). Energy expenditure is also an important determinant of whole body fuel metabolism and can be modified after various bariatric procedures in mice [6,32–36]. To decipher the potential consequences of the EGA procedure on whole body energy regulation, both locomotor activity and 24 h energy expenditure were assessed 30 days after surgery. We found that the surgery had no significant effect on locomotor activity either during the day or at night (suppl Fig. 1c). In addition, respiratory exchange ratios (RER) and total energy expenditure (EE) were similar in both groups (suppl Fig. 1d, e). Collectively, these data demonstrate that, in contrast to previous observations in high fat diet-fed mice[13], *ob/ob* mice are resistant to the modifications in food intake, body composition and energy expenditure induced by the EGA procedure in wild-type animals. This model thus provides a useful system to disentangle the effects of surgery-induced weight loss versus altered glucose metabolism.

3.2. EGA procedure normalizes glucose homeostasis in ob/ob mice despite unchanged whole-body insulin resistance

Bariatric procedures are known to improve glucose homeostasis [37,38]. Basal glycemia was significantly decreased in EGA-ob compared to sham-ob mice during the follow-up period (Fig. 1c). We previously demonstrated that the EGA procedure reduced insulin resistance in the high fat diet-fed mouse model [13]. Contrasting with these observations, HOMA-IR index and intraperitoneal insulin tolerance test (IPITT, 0.75 UI/kg of insulin) results were similar in *ob/ob* mice before surgery (ob-ob), in EGA-ob mice and in sham-ob mice at the end of the follow-up, suggesting a weak effect of the EGA procedure on insulin sensitivity in *ob/ob* mice (Fig. 1d-e). Most importantly, excursions in glycemia during an oral glucose tolerance test (OGTT) in EGA-ob mice performed one month after surgery were similar to those of lean mice, and significantly different from those of animals prior to surgery (ob-ob) and to sham-ob mice (Fig. 1f-g). This major improvement in glucose homeostasis was linked to a significant increase in insulin and C-peptide levels during the glucose challenge (Fig. 1h–i), suggesting that EGA enhances the secretory capacity of beta cells. Moreover, the shape of the post-surgical glucose curve during OGTT paralleled that of lean mice, suggesting that the EGA procedure lowered the threshold for a response to glucose (i.e. increased the glucose sensitivity) of beta cells, and/or corrected the kinetic parameters of insulin secretion (Fig. 1f). We therefore performed a 2UI/kg IPITT (suppl Fig. 1f). By using this dose of insulin, we intended to reproduce the peak of insulinemia during the OGTT (30 ng/ml at time 15mn, Fig. 1f, suppl Fig. 1g). Nevertheless, as early time points weren't collected and as insulin kinetic could be different between IPITT and OGTT, it is noteworthy that insulin peak could be different during the IPITT, possibly even higher. This revealed that the decrease of blood glucose levels was similar between sham and

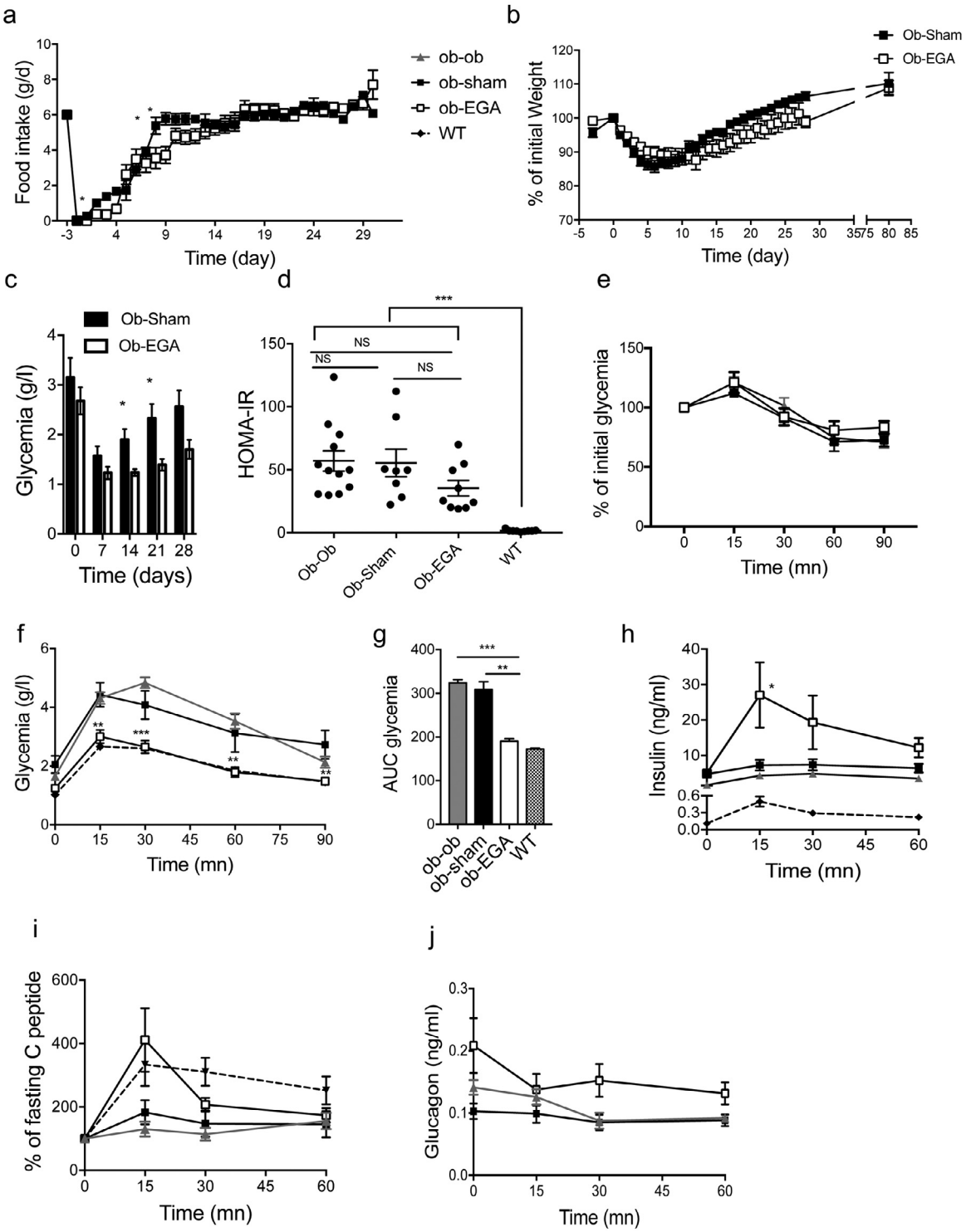

Fig. 1. Effects of EGA procedure on body weight and systemic inflammation and glucose homeostasis in *ob/ob* mice.

a: Daily food intake (g/day; $n = 17-18$ per group), b: Percentage of initial body weight ($n = 17-18$ per group), c: Morning basal glycaemia ($n = 11-15$), d: HOMA-IR insulin resistance index 30 days after surgery, e: intraperitoneal insulin tolerance test (IPITT) after injection of 0.75 units/kg of insulin aspart ($n = 9-10$). f: Oral glucose tolerance test (OGTT 1.5 g/kg) ($n = 8-9$), g: Area under the curve during OGTT, h: Insulin secretion (ng/ml) during OGTT ($n = 8-9$), i:% of fasting C peptide during OGTT ($n = 4-8$), j: Glucagon secretion during OGTT ($n = 12-15$). Data are presented as mean ± SEM (* $p<0.05$, ** $p<0.01$, *** $p<0.001$ by ANOVA).

EGA-ob mice, suggesting that EGA does not improve whole body insulin sensitivity (suppl Fig. 1f). Despite a tendency for higher blood glucagon levels in the fasting state in EGA-ob mice, blood glucagon levels during OGTT were similar in *ob/ob* mice before surgery, in sham-ob mice and in EGA-ob mice (Fig. 1j).

Overall, these observations indicate that the EGA procedure promotes a significant improvement in pancreatic beta cell function which is independent of body weight. EGA thus leads to major improvement of glucose homeostasis despite persistent insulin resistance.

3.3. Modest contribution of GLP1 in diabetes amelioration in ob/ob mice post EGA

Bariatric procedures often lead to enhanced GLP-1 secretion and action in rodent models and in human subjects with T2D [7–9]. Thus, increased GLP-1 may be critical for the improvement in beta cell function observed after bariatric surgery. We therefore measured circulating levels of active GLP-1 in the basal state and during OGTT. EGA surgery failed to restore GLP-1 secretion during OGTT in *ob/ob* mice in contrast to previous observations in wild type C57BL6J mice (suppl Fig. 2a and b). However, blood GLP-1 levels are not predictive of GLP-1 action. Therefore, we studied the consequences of whole body reduction of GLP-1 action by a continuous intra-peritoneal infusion of the GLP-1 antagonist, exendin [9–39] amide (Ex 9–39) (or saline), for 28 days in EGA-ob mice[13].

First, systemic blockade of GLP-1 action did not modify the changes in body weight and food intake in EGA-ob mice in comparison to EGA-ob mice infused with saline (suppl Fig. 2c, d). Second, glucose excursion during OGTT in EGA-ob mice infused with GLP1 antagonist was similar to that in mice receiving saline control (suppl Fig. 2e, f). Furthermore, the peak of insulin secretion during OGTT was reduced after Ex9 administration but did not reach the level of Ob-Sham mice (suppl Fig. 2g, h). Finally, circulating levels of active GLP-1 were increased after glucose gavage but not in the fasting state when GLP-1 receptor was blocked by using an antagonist (suppl Fig. 2a). Therefore, our observations suggest that GLP-1 probably has only a minor role on diabetes resolution in our model of EGA in *ob/ob*, mice as previously found in a model of sleeve gastrectomy [10].

3.4. Significant increase of insulin content in pancreas islets post EGA in ob/ob mice

We next studied the anatomical changes occurring in the endocrine pancreas of EGA-ob mice cured for diabetes and in sham-operated mice that remained hyperglycemic. In agreement with previous reports [39,40], pancreatic islets of *ob/ob* mice were found to be extremely large (suppl Fig. 3a-c) but containing a relatively low level of insulin, as assessed by immunochemistry (suppl Fig. 3a, b, d) or immunofluorescence staining (Fig. 2a) [39,41]. Providing one possible explanation for the apparent dichotomy between islet size and islet insulin content, it has previously been demonstrated that, during the adaptive response to insulin resistance in *ob/ob* mice, the insulin secretory rate exceeds the biosynthetic rate, leading to a progressive depletion of insulin stores [42]. Improvement of glucose tolerance was associated with insulin content in pancreatic islets of EGA ob-mice (Fig. 2b-c) along with the insulin-positive area (suppl Fig. 3c-d). Interestingly, both *Ins1* and *Ins2* gene expression in EGA-ob islets was not significantly different from that in sham-ob islets (Fig. 2d) despite being higher than in C57BL6J lean islets. Thus, the increase in insulin content observed after surgery is probably not the consequence of a rise in *Ins1/2* gene expression.

We next questioned if bariatric surgery raises islet insulin content by enhancing beta-cell proliferation. Immunocytochemical analysis showed that EGA surgery did not affect the number of islets/unit area nor pancreatic islet size distribution in *ob* mice (suppl Fig. 3e, f). Islet cellular composition of EGA-ob and sham-ob mice were analyzed by a flow cytometry gating strategy (FACs) that differentiates alpha, beta and a third population ("other cells") including Polypeptide P- and somatostatin-positive cells (Fig. 2e). In comparison to those of sham-ob mice, the islets of EGA-ob mice were characterized by a lower percentage of insulin$^+$ cells and a modest but significantly higher percentage of glucagon+ cells (Fig. 2f), suggesting that the EGA surgery does not induce beta-cell proliferation. This conclusion is further supported by the presence of a similar number of Ki67$^+$/insulin$^+$ cells in both groups (Fig. 2g). In addition, no proliferation of glucagon$^+$ cells was observed after surgery (Fig. 2h). Thus, the change in alpha- to beta-cell ratio after EGA surgery is unlikely to be caused by beta-cell dedifferentiation. In fact, although we did detect an decrease in the expression of *Aldh1a3* and *Serpin 7*, markers of beta cell de-differentiation in diabetes [43] in islets from EGA-treated mice, the expression of key beta-cell signature genes (*Pdx1, Foxo1, Pax6, Nkx6–1, Mafa*) and beta-cell "disallowed" genes (*Slc16a1*/*MCT-1, Ldha*) [44–46] was similar in islets of both groups (Table S2). In summary, EGA enhanced pancreatic insulin content independently of changes in *Ins1/2* gene expression, beta-cell proliferation or differentiation, further suggesting that other mechanisms lead to an increase in insulin synthesis and secretion.

3.5. Systemic and intra-islets inflammation are unchanged after EGA in ob/ob mice

Accumulating evidence points to tissular and systemic low-grade inflammation as a primary driving force for the development of insulin resistance and beta-cell dysfunction [47,48]. Since low-grade inflammation is a hallmark of *ob/ob* mice [49], and is related to islet dysfunction in type 2 diabetes [50], we examined systemic and beta-cell inflammation patterns in our model. Circulating levels of interleuin-6 (IL-6), Tissue necrosis factor-α (TNFα), resistin and monocyte chemoattractant protein-1 (MCP-1) levels were not significantly different in EGA-ob compared to sham-ob mice, demonstrating persistence of systemic low grade inflammation (suppl Fig. 4a-d). We next assessed the percentage of CD45$^+$cells per islet by fluorescence-activated cell sorting (FACS) and observed no difference between sham and EGA-ob mice (suppl Fig. 4e). Finally, the expression of *IL-6* and *IL-1β* genes was similar in islets of both groups, suggesting that EGA surgery does not improve systemic or intra-islet inflammation (suppl Fig. 4f).

Ob/ob mouse islets are characterized by increased endoplasmic reticulum (ER) stress [49]. In agreement with the lack of beneficial effects of EGA procedure on inflammation, the expression of genes involved in ER stress was not significantly changed after the procedure (suppl Fig. 4g). Taken together, these observations indicate that local pancreatic and systemic inflammation do not explain the improved glucose tolerance of *ob/ob* mice following EGA surgery.

3.6. EGA surgery in ob/ob mice induces major changes in beta-cell gene expression profile

To determine whether other transcriptomic changes may contribute to the effects of EGA on insulin secretion, we compared the global gene expression profile of pancreatic islets of EGA-ob mice, sham-ob mice and C57BL6J wild type lean mice. Microarray analysis of the islet transcriptome of EGA-ob and sham-ob mice identified 458 genes differentially expressed between the two groups (logFC $>$ 1 and $<$ −1, corrected p value $\leq$ 0.05, FDR$\leq$0.001 as thresholds) (Fig. 3a, suppl Fig. 5a). After manually removing the probes without gene names, and genes with unknown physiological functions in beta cells, 193 genes were differentially expressed between EGA-ob and sham-ob mice (suppl Fig. 5b). Expression of 15 of these was confirmed by qPCR (Fig. 2d, suppl Fig. 4f-g, suppl Fig. 5d). Among the top 30 up- or down-regulated genes differing between EGA-ob and sham-ob mice, surgery affected the level of several genes linked to important beta-cell functions such as insulin secretion (*Trpm5, Txnip, Cnr1, Gad1, Kcnf1, Aldob, Ptger3, Calb2, Cartpt, Kcnk10),* survival (*Nnat, Dbp, Olfm1)* and proliferation *(Fos, Reg3b, Reg2, Rgs8, Rgs16)* (Fig. 3b, Table S3 and S4). We noticed that after the EGA procedure expression genes likely to alter insulin secretion or beta cell survival (such as *Txnip, Arrdc4, Rgs8, Rgs16, Sik1, Sv2c, Cxcl10* and *Dapk2*) was reduced. Lastly, the EGA procedure down-regulated genes with unknown roles in beta cell physiology (*Akap12, C1qtnf1, Kcnk10, Slitrk3* and *Gins2*). Additionally, no change in the expression of GLP-1R (*Glp1r*), glucagon (*Gcg*) or of prohormone convertase 1/3 (pcsk1) was observed after EGA

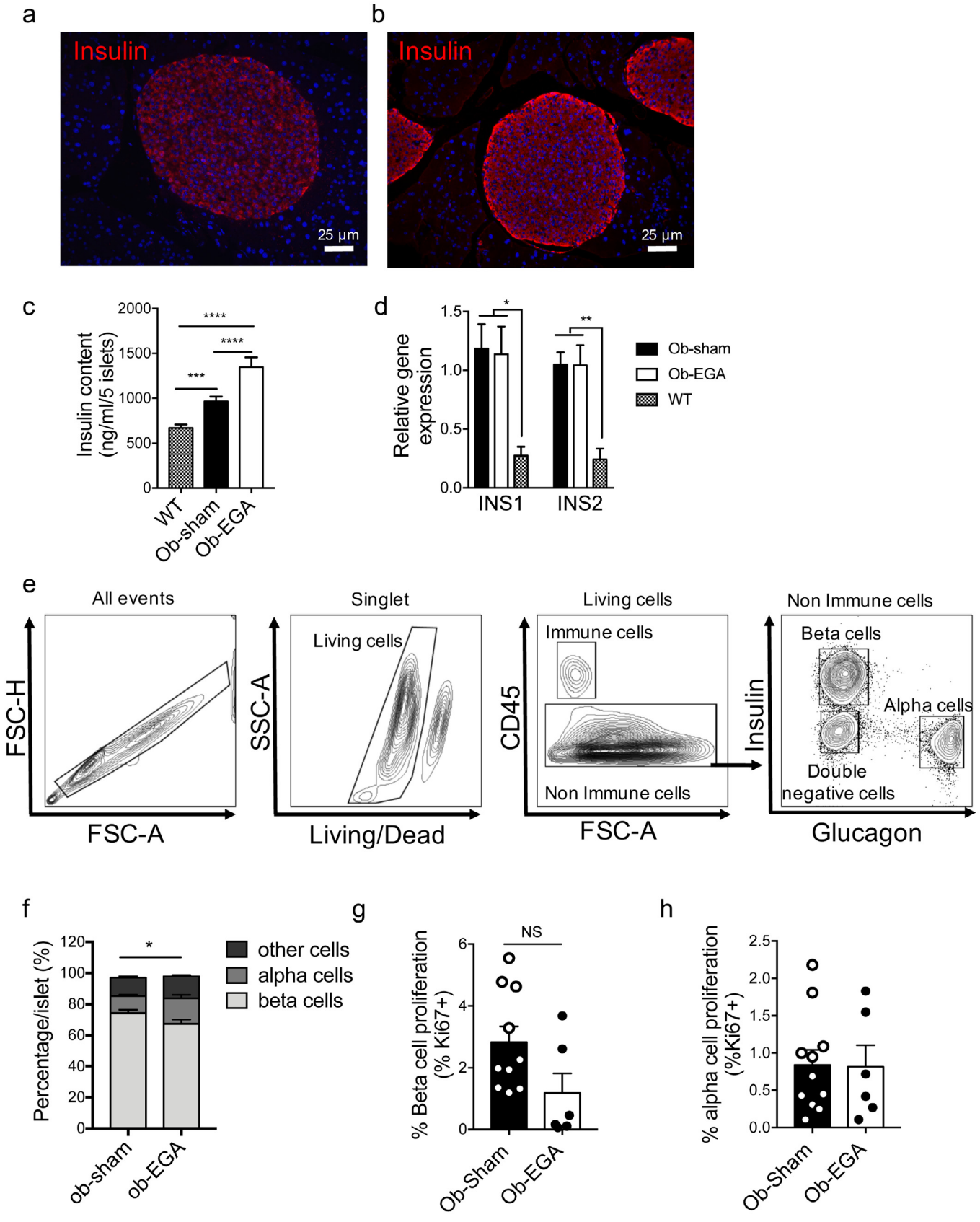

Fig. 2. Changes in endocrine pancreas morphology, islet cell repartition and expression of beta-cell differentiation genes following EGA surgery.

a, b: Immunostaining for insulin (red) in EGA-ob mice 30 days after surgery (x100), Hoechst in blue. c: insulin content in five islets of sham-ob mice and EGA-ob mice and WT mice ($n = 3–6$). d: *Ins1* and *Ins2* gene expression at the end of the follow-up (qPCR fold change vs Sham normalized by 18S, cyclin A, beta actin) ($n = 7–9$), e: Flow cytometry plot showing the gating strategy for immune cells, beta cells, alpha cells and insulin / glucagon double-negative cells obtained from islets of C57BL6J mice ($n = 11–7$) f: Beta and alpha cell separation in pancreatic islets of ob-Sham and ob-EGA G-H: Beta (g) and alpha (h) cell proliferation (proportion of Ki67 positives cells). Data are presented as mean ± SEM ($^{*}p < 0.05$ $^{**}p < 0.01$, $^{***}p < 0.001$ by ANOVA or Mann and Whitney test).

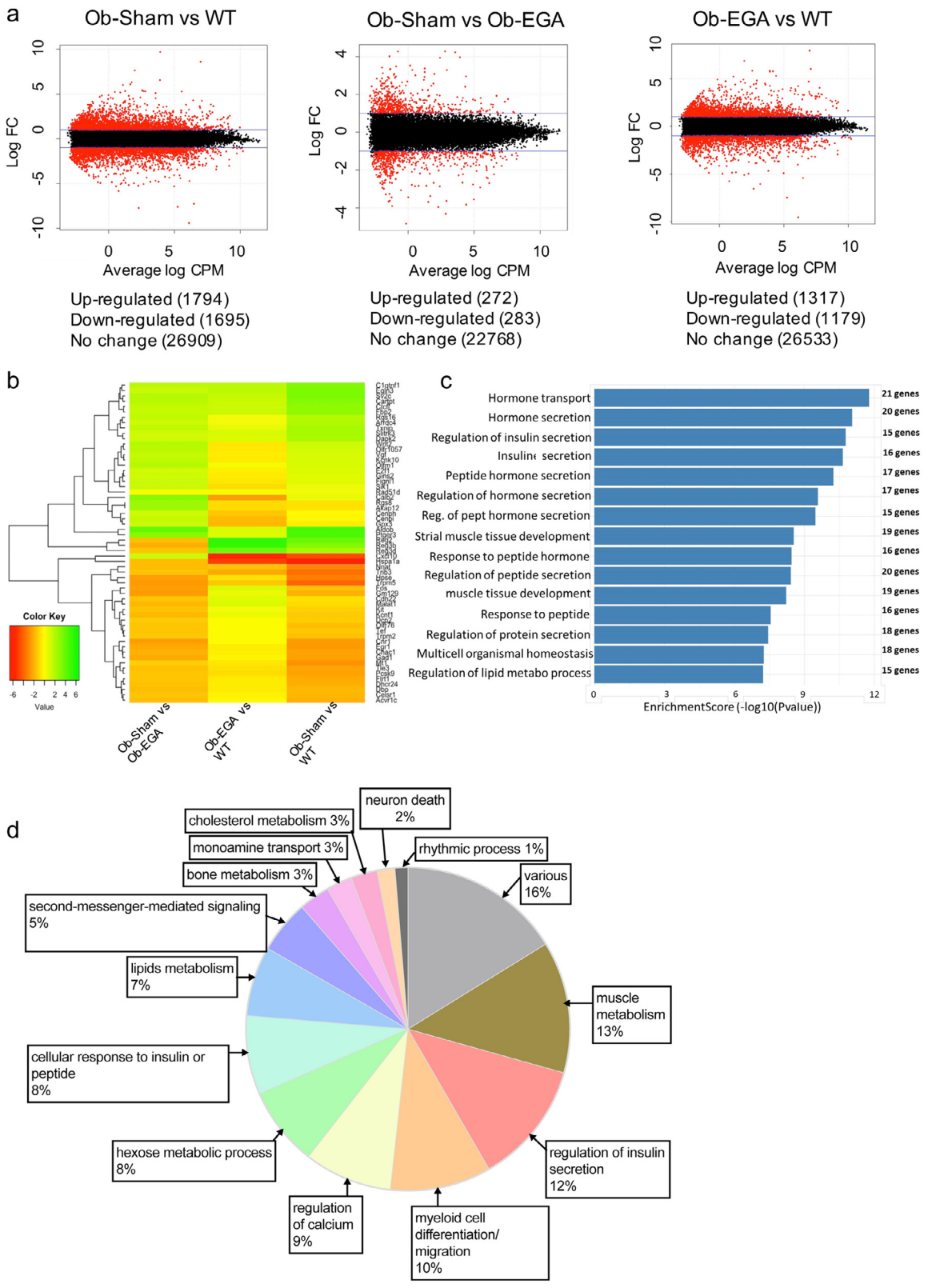

Fig. 3. Molecular analysis of islets after the surgery.

a: Volcano Plots showing genes differentially expressed in pancreatic islets of C57BL6J wild type (WT), sham ob mice and EGA-ob mice (logFC > 1 and < -1, p-value ≤ 0.05, FDR ≤ 0.001 as thresholds). b: Heat map analysis of the 30 up- and −down regulated genes after the surgery for C57BL6J wild type, sham-ob mice and EGA-ob mice. c: Genes regulated by the surgery in sham- and EGA-ob mice are enriched for beta cell function-related of the GO term. Significant pathway enrichments of the 193 differentially expressed genes is shown as the −log10 (enrichment p-value). d: Distribution of 227 enriched pathways according to their functions.

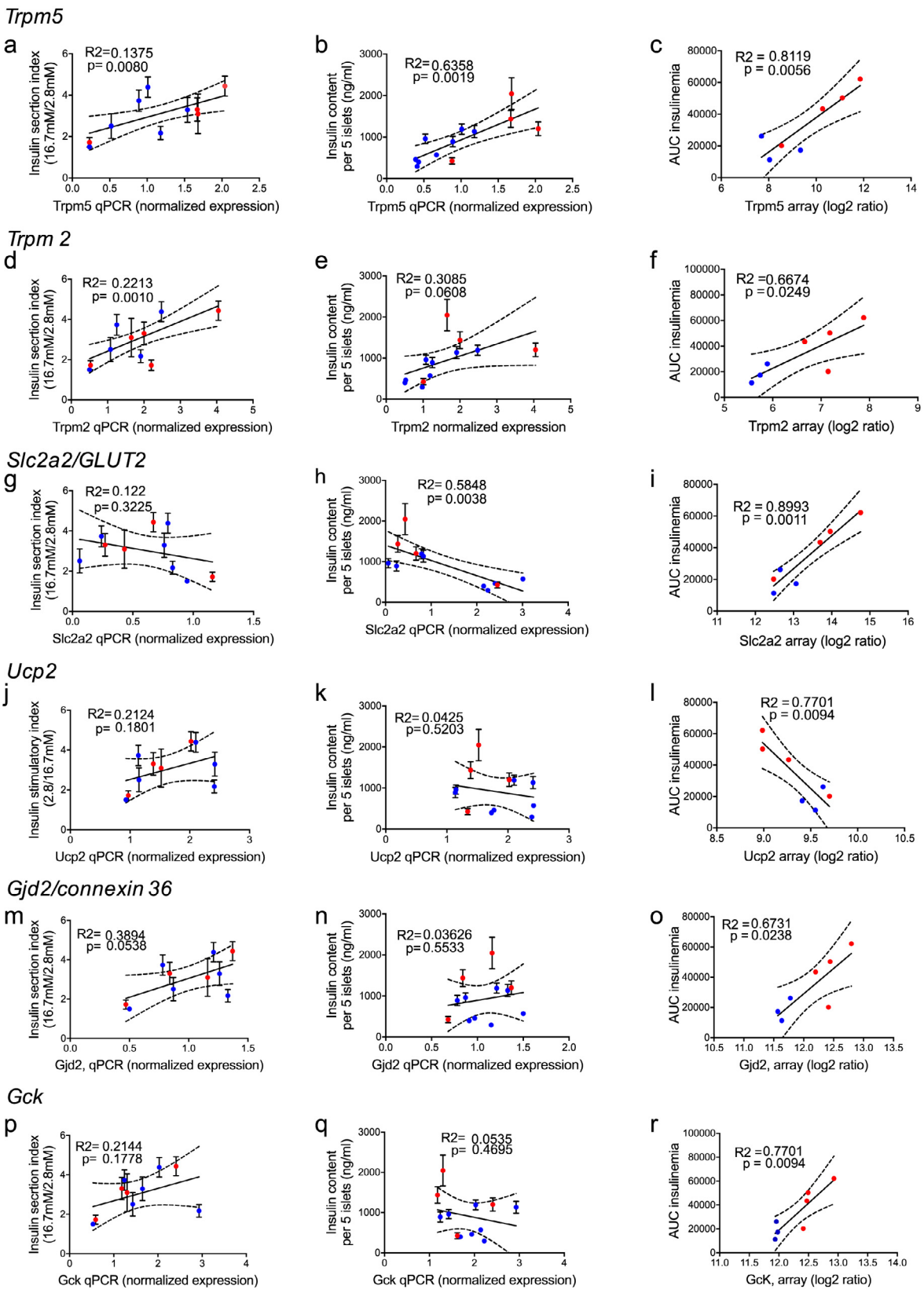

Fig. 4. Correlation between beta-cell function and gene expression after surgery.

Linear regression between insulin secretion index from isolated islets (16.7/2.8 mM), quadruplicate measures per animals (a, d, g, j, m, p), insulin content per five islets (b, e, h, k, n, q), quadruplicate measures per animals and AUC insulinemia during OGTT (1.5 g/kg body weight) (c, f, i, l, o, r) with *Trpm2, Trpm5, Glut2* (*Scl2a2*), *Ucp2*, connexin 36 (*Gjd2*) and glucokinase (*Gck*) expression in islets (qPCR or array intensities). In blue are the Ob-sham animals and in red are the Ob-EGA animals.

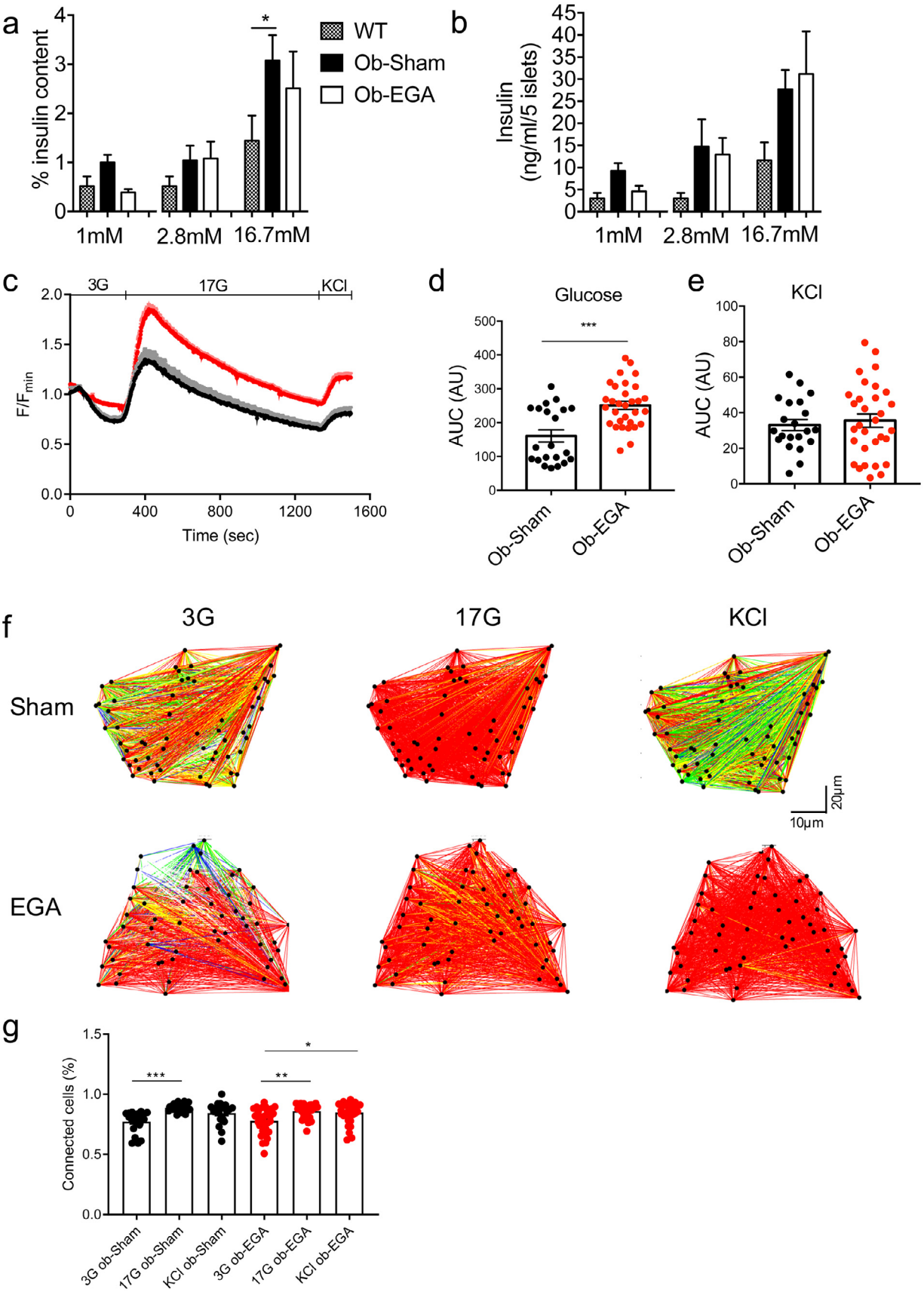

Fig. 5. Functional analysis of beta-cells after the surgery.

a and b: Glucose-stimulated insulin secretion in isolated islets from WT, EGA- and Sham-ob mice. Data are expressed as% of insulin content (a) and absolute values (b) ($n = 15–20$ islets per animals isolated from 3 to 5 animals in response to low (3 mM), high (17 mM) glucose). c: Intracellular Ca^{2+} responses from Sham ($n = 21$) and EGA ($n = 31$) islets isolated from three mice each in response to low (3 mM), high (17 mM) glucose or 20 mM KCl. EGA increased both the amplitude and (d) the area-under-the-curve of glucose-

(respectively, p value: 0.114, FDR: 0.375 and p value: 0.593; FDR: 0.828, p value:0.03, FDR: 0.161). Interestingly, when compared to the islets of C57BL6J wild type mice, 105 of the 193 selected genes returned to normal levels after surgery, suggesting that the EGA procedure tends to restore a normal gene expression pattern.

Next, we performed a Gene Ontology (GO) Term enrichment analysis and identified 227 biological processes significantly modified after surgery (enrichment adjusted p-value < 0.05). The most enriched group included 21 genes (*Cnr1/Nnat/Acvr1c/Trpm2/Sox4/Hmgcr/Pim3/Adora1/Gipr/Sytl4/Ccl5/Adora3/Aqp1/Tiam1/Gpr68/Arntl/Serpina7/Vgf/C1qtnf1/Cartpt/Ptger3*: "hormone transport", GO term identification number: GO:0009914), which play a substantial role in the regulation of insulin secretion (Fig. 3c, Table S5). Classification of 227 biological processes by functional categories are represented in Fig. 3d. Intriguingly, 30 biological processes (13% of the total) were associated with striated muscle metabolism / muscle cell differentiation. This finding was unexpected. The most differentially enriched group (called "striated muscle tissue development", GO GO:0014706) included 19 genes (*Fos/Egr1/Nr4a1/Actn3/Cyp26b1/Rgs2/Hspg2/Hmgcr/Nr1d2/Rara/Dsg2/Tpm1/Hdac9/Ppara/Arntl/Atf3/Cdk1/Sik1/Wnt2*). Comparison of "hormone transport" and of "striated muscle tissue development" biological processes showed only one common gene (*Hmgcr*). A literature search revealed that 13 of the 19 genes included in the "striated muscle tissue development" biological process (GO-BP) group have an established role in beta cell physiology and insulin secretion (Table S5). Thus, we propose that this biological process (and the additional 29 regulated genes in the same GO term family) can be added to the 28 biological systems linked to insulin secretion. In summary, EGA surgery in *ob/ob* mice modifies the expression of several islet genes involved in multiple molecular pathways and, particularly, in the regulation of insulin secretion. These changes are therefore likely to contribute to the improved glucose homeostasis observed after EGA surgery.

3.7. Relationships between islet genes and rescued beta-cell functionality in ob/ob mice post EGA

Ob/ob islets are characterized by impaired ATP generation (and increased islet expression of *Ucp2* [41]), altered beta-cell-beta cell coupling (and reduced connexin 36 *(Gjd2)* expression [51]), and the down-regulation of genes involved in the early metabolic steps required for the triggering of insulin secretion by glucose, notably reduced *Slc2a2* (*Glut2*) and *Gck* expression [42,51]). The transcriptomic changes observed in islets after the EGA procedure seem likely to contribute to the correction of some of these defects. Thus, *Trpm5* was the most up-regulated gene in pancreatic islets after EGA (suppl Fig. 5d, Table S3). We showed that GSIS in vitro and in vivo, as well as islet insulin content, were strongly correlated with *Trpm5* expression (Fig. 4a-c). The highest expression of *Trpm5* (as observed in EGA-ob mice) correlated with the highest beta-cell functional capacities both in vivo and in vitro. This relationship was also observed for the *Trpm2* gene, suggesting that the TRPM family of ion channels is regulated by EGA surgery and is an important contributor towards beta-cell recovery both in vitro and in vivo (Fig. 4d-f, suppl Fig. 5d). Enhanced insulin secretion in vivo was also correlated with up-regulation of the *Gck, Slc2a2*/*Glut2* and *Gjd2*/connexin36 genes and with down-regulation of *Ucp2*, in EGA-ob mice (Fig. 4i, l, o, r).

Another defect observed in *ob/ob* islets is that basal insulin secretion at 2.8 mmol/l glucose was significantly elevated when compared to lean animals [41]. In contrast, insulin secretion was nearly constant when glucose increased from 11 to 22 mmol/l in *ob/ob* mice. The shift of the glucose dose-response curve to lower glucose concentrations as observed in *ob/ob* mice has been explained by higher mitochondrial activity at low glucose levels, and contributed to the depletion of islet insulin content [51]. Interestingly, the sensitivity to extremely low glucose levels (1 mM) for insulin secretion in ob-sham islets in vitro, seems to shift towards higher glucose levels after EGA surgery, suggesting changes in the threshold for GSIS (Fig. 5a, b). As a consequence, it could be postulated that inappropriate insulin secretion at low glucose levels (one of the well characterized defects of pancreatic islets of *ob* mice [51]) is reversed, contributing to the increased insulin content observed after the EGA procedure.

Ob/ob islets are also characterized by loss of high frequency glucose-induced intracellular Ca^{2+} oscillations, partly explained by down-regulation of the nonselective cation channel *Trpm5* [52]. Previous analysis [53,54] of intracellular Ca^{2+} signals in individual beta-cells within pancreatic islets also showed that cell-to-cell coupling was reduced in *ob* mice compared to controls. We therefore questioned whether EGA surgery might modify this defect. Ca^{2+} imaging using the intracellularly-entrapped fluorescent probe Cal-520 (see Methods), revealed that islets from EGA-ob mice responded with an enhanced oscillatory increase in intracellular Ca^{2+} free concentration during stimulation with 17 mM glucose in comparison to sham-ob mice (Fig. 5c, d). In contrast to this action on the effects of high glucose, intracellular Ca^{2+} increases in response to depolarization induced by a short pulse of KCl were similar in both groups (Fig. 5c, e). The latter finding supports the view that increased Ca^{2+} signals in EGA-ob mice may be mediated by changes in glucose metabolism upstream of Ca^{2+} influx. In both groups, cell-to-cell coupling among beta-cells, and the proportion of interconnected cells, increased similarly in response to an increase in glucose from 3 to 17 mM or during KCl stimulation (Fig. 5f, g), despite increased *Gjd2* expression (Fig. 4o). In summary, glucose-related Ca^{2+} signaling in EGA-ob mice was characterized by enhanced responses to elevated glucose, but unchanged cell-cell coupling, when compared with sham-ob mice. These data are consistent with increased intracellular glucose metabolism, and a lowered threshold for GSIS, as expected after increased expression of *Glut2* (*Slc2a2*) and *Gck* (Fig. 4i, r) (and possibly a lowering in *Ucp2*; Fig. 4l), in *ob/ob* islets after EGA.

3.8. EGA surgery changes the miRNA expression profile of pancreatic islets

MiRNAs are translational repressors that play a major role in the control of gene expression. They have emerged as important regulators of beta cell function and display expression changes under obesity and diabetes conditions [55–57]. To assess whether these small non-coding RNAs contribute to the mechanisms by which beta-cell function was dramatically improved in the EGA-ob mice group, we next performed global miRNA expression profiling of islets from EGA-ob and sham-ob mice. We were able to analyze the expression of 417 miRNAs in these two conditions. We found that 22 of the 417 detected miRNAs were up-regulated in EGA-ob islets (extreme fold change from 25 to 1.27, adjusted p-value <0.05) whereas five were down-regulated (extreme fold change from −1.58 to −1.42, adjusted p-value <0.05) (Fig. 6a, Table S6). The changes in the expression of several of these miRNAs were confirmed by qPCR (Fig. 6b) and were also compared to islets of C57BL6J lean mice. Interestingly, EGA surgery in *ob/ob* mice normalized the expression in islets of several

evoked Ca^{2+} traces (AUC; $^{***}p<0.001$) but not (e) the depolarizing stimulus, KCl. Data are means±SEM. f: Cartesian functional connectivity maps displaying the x-y position of analyzed cells (black dots). Cells are connected with a line where the strength of each cell pair correlation (the Pearson R statistic) is color coded: red for R of 0.76 to 1.0, yellow for R of 0.51 to 0.75, green for R of 0.26–0.5 and blue for R of 0 to 0.25. Results are shown at low (3 mM), high Glucose (17 mM) or 20 mM KCl for each of the mouse groups during the imaging period. g: The percentage of significantly connected cell pairs increases under high glucose concentrations in both groups and under KCl in the EGA-ob mice. No difference between the groups was detected. Data are presented as mean ± SEM and $^{*}p<0.05$, $^{**}p<0.01$, $^{***}p<0.001$ following 1-way ANOVA.

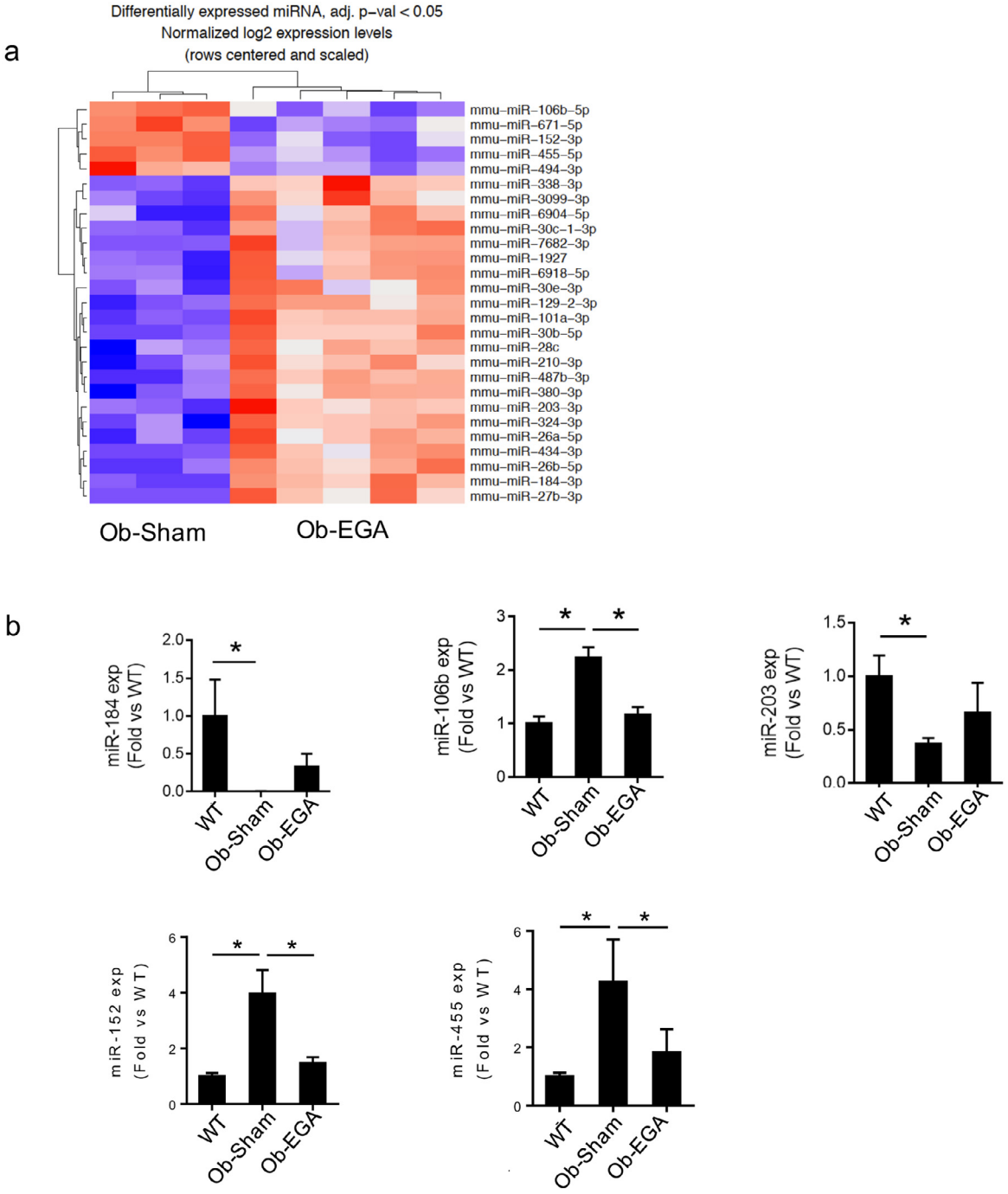

Fig. 6. Changes in islet miRNA expression profile after surgery.

a: Heat map of 27 miRNAs significantly differentially expressed into the islet of EGA-ob mice compared to those of Sham-ob mice. b: qPCR confirmation of miRNA-184−3p, miRNA106b, miRNA-203, miRNA-152, miRNA-455 expression in the islet of C57BL6J mice and Sham and EGA-ob mice. Data are presented as mean ± SEM (*$p < 0.05$ by Mann and Whitney test).

miRNAs, including a number previously known to be dysregulated in different obese mouse models [56,58–61] (Fig. 6b).

3.9. Integration of miRNAs and gene array data set from EGA-ob mice islets

We next performed a computational analysis to unravel the interactions between the 27 miRNAs and the 193 genes differentially expressed after surgery. First, bioinformatic analysis predicted that 15 of the 27 miRNAs (miR-30c-1−3p, 380−3p, 434−3p, 671−5p, 6904−5p, 7682−3p, 324−3p, 26b-5p, 494−3p, 1927, 106b-5p, 338−3p, 26a-5p, 6918−5p and 3099−3p) regulate the biological process “hormone transport” (GO:0009914) that was the most enriched after surgery (Table S7).

MiRNAs provide a key and powerful tool in gene regulation and mediated translational repression. By using the miRNA target prediction database (TargetScanMouse), we developed an interaction network between the 22 up-regulated miRNAs and the 91 downregulated genes after EGA, predicted to be their targets and between the five downregulated miRNAs and their 102 upregulated predicted target genes (Fig. 7a, b). We demonstrated that up-regulated miR-324−3p, miR-7682−3p and miR-6918−5p had greater than 21, 20

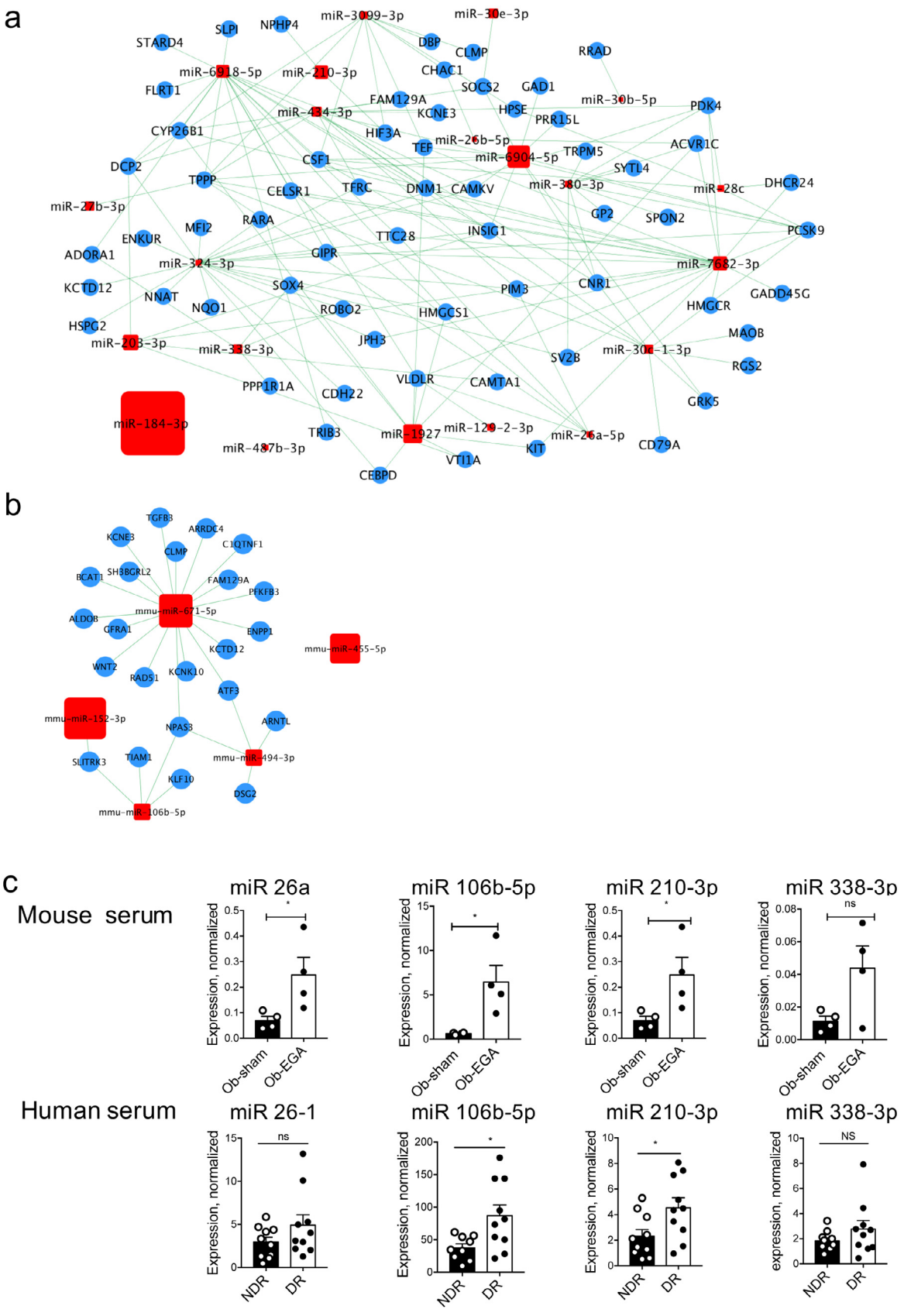

Fig. 7. Blood miRNA signature after surgery.

a: Network between up-regulated miRNAs and down-regulated genes that are predicted to be their targets. b: Network between down-regulated miRNAs and upregulated target genes. c: Circulating miRNAs measured by qPCR in mice serum ($n = 4$ per group) and human serum ($n = 10$ per group). NDR: non diabetes remission, DR: diabetes remission. Data are presented as mean ± SEM ($^*p < 0.05$ by Mann and Whitney test).

and 18 negatively-correlated predicted genes respectively (suppl Fig. 6). Similarly, down-regulated miR-671−5p has more than 18 positively-correlated predicted genes (suppl Fig. 6). This suggests that affected miRNAs are central nodes of miRNA-gene interaction networks and may be important regulators of gene expression in beta cells during the remission of diabetes after bariatric surgery. Going a step further, we questioned to what extent these regulations were specific to bariatric surgery. Towards this aim, we analyzed changes in miRNA expression in pancreatic islets in ob mice in another situation of metabolic improvement, the administration of leptin. As expected, leptin administration reduced body weight, insulin resistance, and circulating IL-6 as well as normalizing glucose tolerance to the level seen in EGA ob mice (Suppl Fig. 7a-e). Of 386 miRNAs detected in pancreatic islets, 73 were up-regulated and 60 were down-regulated after the administration of leptin (suppl Fig. 7f). Among them, only 14 miRNAs were regulated to the same extent as observed in EGA-ob mice (13 up-regulated and one down-regulated) (suppl Fig. 7f, g). Additionally, among the four miRNAs that contribute to the regulation of the largest panel of the 193 genes of interest in EGA-ob mice, miRNA 671−5p was the only one differentially regulated in leptin-treated ob mice. In summary, leptin treatment has unique effects on the islet miRNA signature and EGA partially replicates these effects. This suggested that despite similar metabolic improvement, EGA regulated miRNAs expression by specific mechanisms.

3.10. Identification of a miRNAs signature in blood correlated with diabetes remission in humans

Circulating miRNAs have been suggested to be promising biomarkers for a wide variety of human pathologies, including diabetes [62−64]. In this context, translational studies are made possible because miRNAs are highly conserved among species. We investigated how a subset of miRNAs was associated with diabetes remission in humans after bariatric surgery. To this end, we compared in mouse and human blood samples the expression of four miRNAs among the 27 miRNAs differentially expressed in pancreatic islets of EGA-ob mice (known to be well conserved between species, highly expressed in beta cells and to circulate in blood). To avoid a potential effect of weight loss on circulating miRNA levels, we choose 20 patients from the French BARICAN cohort [65] who underwent gastric bypass and separated them into two groups depending on whether, one year after surgery, they showed T2D remission (DR) or not (NDR) as defined by the American Diabetes Association (ADA) [18,19]. All patients had similar pre- and post-surgery body mass index (BMI). These and other characteristics are listed in Table S8. The differences in miRNA levels in the blood of 10 DR and 10 NDR patients were tested and compared to those observed in the blood of Sham and EGA-ob mice. We found that the expression of miR-26a-5p, miR-106b-5p, miR-210−3p were similarly up-regulated in blood upon diabetes remission in *ob* mice and in humans (tendency for miR-26a in humans) (Fig. 7c). On the other hand, circulating levels of miR-338−3p were unchanged both in mice and in humans. Our results thus provide evidence for a blood-miRNA signature associated with diabetes remission in *ob/ob* mice and humans.

4. Discussion

The present study identified a molecular signature in pancreatic islets and in blood related to diabetes remission after bariatric surgery in diabetic *ob/ob* mice and in humans. The various forms of bariatric surgery (especially those with a malabsorptive component such as Biliary Pancreatic Diversion with Duodenal Switch) improve insulin secretion and insulin sensitivity [66−68]. We hypothesized that one way to identify specific new mechanisms affecting pancreatic islets after bariatric surgery was to minimize the contribution of confounding factors such as the reduction of food intake and body weight. We took advantage of *ob/ob* mice in which we showed that resolution of diabetes after bariatric surgery was independent of changes in diet and body weight, as previously described [69]. In contrast, Mokadem et al. [70] showed that RYGBP is able to reduce body weight in *ob/ob* mice but fails to restore normal glucose homeostasis, suggesting that leptin is important for the regulation of glucose levels and not for the regulation of body weight in the post-surgical period in this case. These differences with our results may be explained, first, by differences in surgical technique since Mokadem et al. performed a Roux-en-Y reconstruction of the gastrointestinal tract with two anastomosis (distal transected jejunal limb to the proximal anterior gastric wall and the proximal transected jejunal limb to the afferent Roux limb). Our results also differed from those of Mokadem et al. in the post-operative time course (6−7 weeks versus 28 days in our study) which is characterized by a progressive increase of glycemia over time and possible reduction of meal-stimulated incretin and insulin secretion following the RYGBP in *ob/ob* mice [71]. Hao et al., [69] reported that, in *ob/ob* mice, body weight was reduced by RYGB transiently in the first week, recovered in the second week and increased over the baseline thereafter. These data are similar to our observations, and suggest an important role for leptin for the maintenance of body weight loss after the surgery. Furthermore, and similarly to the study of Hao et al., lack of significant body weight loss probably explained in our study why insulin sensitivity was not improved during the follow-up.

Here, we showed that normalization of glucose excursion after the EGA procedure is driven mainly by an enhancement of insulin secretion and is independent of any significant changes in body weight, food intake, obesity-induced inflammation or insulin sensitivity. In other words, after surgery, beta cells displayed an improved capacity to adapt insulin secretion to a persistently altered metabolic environment. This is all the more remarkable given that lipotoxicity-mediated endoplasmic reticulum stress is a mechanism that contributes to reduced insulin secretion adaptation during obesity development in *ob/ob* mice [49]. We did not find evidence for a reduction of lipotoxicity, nor in intra-islet or systemic inflammation, that could explain the increase of insulin secretion capacity after surgery. Similarly, the distribution of islet cell types was not dramatically modified after the EGA procedure. Consequently, we did not obtain evidence that surgery reverses beta-cell dedifferentiation, except for a small decrease in *Aldh1a3* gene expression [72].

Previous publications emphasized an important role for GLP-1 in the improvement of beta cell function after bariatric surgery [73,74]. Our data suggest that, in *ob/ob* mice, additional mechanisms are at work during diabetes resolution, as previously hypothesized in other rodent models [10,11]. Indeed, we observed that blood GLP-1 levels during OGTT were similar in sham- and EGA-ob mice. Furthermore, despite a reduction of insulin secretion, glucose excursion was not significantly modified after blocking the GLP1 receptor with [9−39] exendin amide, infused for 28 days after surgery. Importantly, exendin [9−39] amide was infused at a rate (2 pmol/kg/min) validated for significant blockade of GLP-1 receptor signaling without non-specific effects [20,21]. Indeed, at the same infusion rate, Cani et al. [20] demonstrated that [9−39] exendin amide reversed the beneficial effects of oligofructose dependent of GLP-1 on insulin secretion, the production of hepatic glucose production and Akt and IR-S2 phosphorylation in the liver. Furthermore, we showed in ob-EGA mice that GLP-1 levels in the blood increased significantly during [9−39] exendin amide infusion suggestive of a positive feedback loop on GLP-1 secretion when GLP-1R function was disrupted with the antagonist (suppl Fig. 2a). A similar regulation of endogenous GLP-1 secretion was also observed in humans during administration of [9−39] exendin amide [75−77]. Taken together, these results suggest that [9−39] exendin amide, at the infusion rate used in our experiments, efficiently blocked GLP-1 receptor function. Because infusion of GLP-1

antagonist had no deleterious effect on metabolic parameters in ob-EGA mice, it can be assumed that changes in GLP-1 play little role in the metabolic improvement after EGA surgery in this rodent model and despite a marked reduction in insulin secretion in the presence of [9−39] exendin (suppl Fig. 2g,h). Our results are similar to those obtained after vertical sleeve gastrectomy in high fat diet-fed mice suggesting that, as in *ob/ob* mice, sensitivity to incretin stimuli may not be enhanced at the receptor expression level as discussed elsewhere [10,78].

EGA-ob mice and lean C57BL6J mice displayed similar glucose excursion patterns during OGTT, despite a significant difference in whole body insulin sensitivity. This is a remarkable effect of EGA surgery if we consider that *ob/ob* mice are characterized by elevated insulin secretion, which is nonetheless insufficient to maintain euglycemia [79], and despite the presence of larger islets of Langerhans [80] with a high proportion of beta cells [39]. Providing a potential explanation for this paradox, morphological analysis of pancreatic islets of *ob/ob* mice revealed beta cells with clear degranulation [39] or weak immunoreactivity for insulin [81]. The latter changes have been proposed to be the consequence of enhanced insulin secretion due to augmented exocytosis at the single cell level at low glucose levels, and reduced ATP production at high glucose level [51]. Here, we show that restoration of beta cell functionality can be ascribed to reduced secretion of insulin from isolated pancreatic islets in response to low glucose concentrations, suggesting a right-shift in the metabolism of glucose and in ATP synthesis. Supporting this interpretation, we demonstrated that islets from EGA-*ob* mice responded with enhanced oscillations (and an overall increase in amplitude) in intracellular Ca^{2+} concentration during stimulation with 17 mM glucose, although the EGA procedure did not change beta cell-beta cell connectivity. This modification may be the consequence of changes in intracellular glucose metabolism and signaling (e.g. enhanced closure of ATP-sensitive K^+ channels) [82] since depolarization induced by a short pulse of KCl was unaffected by surgery. Accordingly, we showed that expression of several important genes of glucose metabolism is changed after the surgery. It is generally accepted that glucokinase *(Gck)* is the key glucose sensor for the regulation of insulin release by pancreatic beta cells [83]. Glucokinase is thus responsible for detecting glucose in the immediate environment of the beta cell. Glucokinase converts glucose to glucose 6-phosphate (G-6-P), an irreversible reaction that determines glycolytic flux where NADH and pyruvate are the primary products, serving as substrates for mitochondrial oxidation. Release of insulin correlates with increases in the rate of ATP synthesis and both parameters increase in response to glucose with a sigmoidal dose response which is similar in rodent and human beta cells [84]. As a consequence, an alteration in *Gck* expression in beta cells can cause mild hyperglycemia (in the case of heterozygous inactivating mutations in *Gck*, as observed in the maturity-onset diabetes of the young (MODY2), subtype glucokinase) or permanent neonatal diabetes mellitus (in the cases of homozygous inactivating *Gck* mutations) or even hypoglycemia [85]. Glucokinase activity is also regulated by Fbp2 (fructose bisphosphatase 2), a gluconeogenic enzyme. Indeed, decreased Fbp2 activity led to reduced fructose 2,6-P(2) content, glucokinase activity and glucose-induced insulin secretion [86]. Thus, the observation in our data that EGA surgery increased *Gck* expression ($p< 0.05$) and decreased *Fbp2* (Table S4) may explain the reduction in beta cell sensitivity at low glucose observed in EGA-ob mice. Additionally, it has been demonstrated that expression of *AldoB* was negatively correlated with insulin secretion in pancreatic islets [87] and that increased expression of *AldoB* in murine islets induced impaired GSIS and ATP production [88]. *AldoB* was the most down-regulated gene in islets from EGA-ob mice suggesting a possible role for this enzyme in the regulation of beta cell function in the context of surgery. Beyond the results above, our data also highlight novel mechanisms of regulation of beta cell functionality important for the resolution of diabetes after bariatric surgery. Thus, transcriptomic analysis of EGA and sham-ob mice pancreatic islets showed that EGA surgery reversed the down-regulation of *Slc2a2/Glut2, Gck, Trpm5, Trpm2* and connexin-36 *(Gjd2)* ($p<0.05$ when compared to sham-ob mice) and the overexpression of *Ucp2* which has been linked to loss of glucose-induced insulin secretion from *ob/ob* beta cells [41], all defects with demonstrated causal role in the reduction of insulin secretion in this model. For example, up-regulation of *Gck* and of *Glut2/Slc2a2* (after a treatment with a sympatholytic dopamine agonist) [42] or up-regulation of pancreatic *Trpm5* by leptin treatment [52], improved high frequency glucose-induced Ca^{2+} oscillations and GSIS. Importantly, during diabetes remission we also highlighted several genes (*Akap12, C1qtnf1, Kcnk10, Slitrk3* and *Gins)* with previously unknown physiological functions in pancreatic beta cells which may potentially be new targets for T2D treatment. If we compare our transcriptomic results with those recently presented by Douros et al. [78], it is intriguing to observe that although VSG and EGA surgeries shared common phenotypic consequences in high fat diet mice and in *ob/ob* mice (increased insulin secretion both in vivo and *ex vivo*, modifications of Ca^{2+} oscillation amplitude and changes of glucose sensitivity in islets), the changes in islet transcriptome were different in the two models. Indeed, even though a significant enrichment was observed for genes involved in the control of insulin secretion and Ca^{2+} signaling pathways in both settings, there were no common enriched genes between the datasets. There are several possible explanations for this difference. First, we studied mice 30 days after the EGA procedure while Douros et al. performed analyses 10−14 days after the VSG. Second, the pathophysiological mechanisms involved in altered islet function in the two models are probably different. As mentioned above, the EGA procedure reversed the main molecular defects present in *ob/ob* islets and one could postulate that it was the same for high fat diet-fed mice after the VSG. Thus, despite differences in phenotype and pathophysiology of obesity in high fat diet and in *ob/ob* mice, both models and both surgeries enrich our knowledge of the molecular defects in islet function and to what extent bariatric surgery may correct them. Altogether, and considering the changes in gene expression, these data suggest that changes in insulin secretion after surgery are at least in part dependent on modifications in beta cell glucose metabolism.

MiRNAs are critical regulators of pancreatic beta cell physiology and some of these small non-coding RNAs are involved in the regulation of insulin secretion [89]. However, publications on the regulation of miRNAs after bariatric surgery provide conflicting results and, for the most part, are based on analysis of miRNAs in blood and not in pancreatic beta cells as performed here. In our study, among the 27 miRNAs differentially regulated in the islets after the bariatric surgery, 15 have no known role in beta cell physiology. Twelve of them were up-regulated and have not previously been implicated in the resolution of diabetes after bariatric surgery. Of the remaining 12 miRNAs, diabetes in humans or rodent models has previously been associated with down-regulation of eight: miR-26b-5p, miR-26a-5p, miR-27b-3p, miR-434−3p in the blood and miR-184−3p, miR-338−3p, miR-203−3p and miR-210−3p in pancreatic beta cells [58,90−92] and up regulation of four: miR-106b-5p, miR-152−3p, miR-30b-5p, miR-101a-3p in pancreatic islets [93−95]. Remarkably, our data show that EGA tended to correct and restore to wild-type levels almost all the other miRNAs known to be dysregulated in pancreatic islets during diabetes in rodent models [56,58−61], except for miR-30b-5p and miR-101a-3.

Interestingly, it has been reported that up-regulation of miR-152−3p observed in diabetic rodent islets reduced expression of *Gck*, ATP availability and GSIS [93]. The down-regulated expression of miR-152−3p after EGA may be linked to the increased *Gck* expression observed in our data set as mentioned above [93]. To further understand the interaction between the regulation of miRNAs and the changes in the level of the 193 genes affected by the surgery, we built

a miRNA-gene interaction network. We found that miRs 324−3p, 671−5p, 6918−5p and 7682−3p stood out as important hubs, each of them regulating between 18 and 21 genes of interest, including *AldoB*. Even if a direct link between these miRNAs and beta-cell physiology is not yet established, our data highlight a potential role for these four miRNAs in the regulation of intra-islet function during the surgery. We next demonstrated that for a similar improvement of glucose homeostasis, changes in miRNAs expression were different after the administration of leptin in ob mice when compared to EGA-ob mice. This suggested that the normalization of glucose levels is not sufficient by itself to explain the alteration expression of miRNAs in pancreatic islets in the two conditions. In addition, because leptin has an important role in post-surgery weight change [69], we cannot exclude that loss of body weight during leptin administration may contribute to the regulation of miRNA expression. Going a step further, we hypothesized that it was possible to determine a miRNA blood signature that correlates with diabetes remission upon bariatric surgery in humans on the basis of our results obtained in *ob/ob* mice. Accordingly, the blood levels of miR-106b-5p and miR-210−3p were similarly increased during diabetes remission after bariatric surgery in humans and in EGA-ob mice and in human a similar tendency was also observed for miR-26a-5p. In contrast, diabetes remission did not affect the circulating level of miR-338−3p either in mice or in humans. These results suggest common mechanisms of regulation for these four non-coding RNAs among species. It is to be noted that most previous studies evaluating the circulating levels of miRNAs after gastric bypass were obtained in non-diabetic cohorts [96−99]. Furthermore, the small number of studies performed on Type 2 diabetes patients after bariatric surgery have compared circulating miRNA levels post-operatively only with the pre-surgery state (which is therefore an obese state) [100−102]. Thus, the differential levels of circulating miRNAs in these cohorts could be a consequence of weight loss rather than diabetes remission. This highlights the strength of our study which was performed on a bariatric surgery rodent model without any weight loss bias (as obesity remained after EGA) or in a bariatric surgery human cohort with different diabetes evolution but similar pre- and post-surgery BMI.

A clinical application of the discovery of this blood signature is the development of biological biomarker reflecting beta cell well-being independently of weight variation. This may help to optimize the care of individual patients with diabetes and provide suitable candidates for bariatric surgery. Indeed, the evolution of diabetes varies between subjects after bariatric surgery. This is partly dependent on the procedure: RYGB allows, for a similar glycemia, more limited use of additional anti-hyperglycemic treatments compared to sleeve gastrectomy [38,103]. Since there is currently no consensus on the best use of hypoglycemic compounds after bariatric procedure [104], the evaluation of beta cell functionality may help in the post-surgical follow up of patients with T2D in order to reduce the hypoglycemic or hyperglycemic events during the post-surgical period if diabetes therapy is not adequately adapted to the evolution of beta cell function. However, variable clearance of insulin depending on bariatric procedure, time after surgery and gut peptides complicates the evaluation of beta cell function [15−17]. Thus, in the era of personalized medicine, measurement of the circulating levels of the four miRNAs discovered here, and conserved across species, could provide an important tool to obtain information on beta cell function.

This study is subject to several limitations. First, the choice of *ob/ob* mice may be questionable considering that it is a monogenic model of obesity and diabetes caused by a lack of leptin production. Although leptin mutation is rare in humans, mutations in the downstream leptin circuitry (e.g. MC4R) are often present in obese patients and reduction of MC4R function reduced the effects of bariatric surgery [105]. In addition, the observation of diabetes resolution in *ob/ob* mice despite persistent obesity may not be considered as a bias but may be helpful to identify the mechanisms of early improvement of glucose control independent of weight loss in humans. Consistent with our hypothesis, we discovered novel mechanisms of beta cell recovery that appear, at least in part, to be conserved among species as illustrated by the common circulating miRNA signature of diabetes resolution in this rodent model and in humans. Another limitation of our study is that, for the most part, our findings are correlative rather than a proof of causality. Nevertheless, our data demonstrate that EGA reverses important defects of *ob/ob* pancreatic beta cells by multiple miRs-genes interactions. Future studies will clarify whether any of these pathways are critical during diabetes remission.

In summary, we have identified a potentially important new mechanism, possibly driven by changes in islet miRNA levels, that is associated with remission of diabetes after bariatric surgery in *ob/ob* mice. The improvements in beta cell function were observed in the face of persistent obesity, hyperphagia and inflammation. Based on our computational analysis and correlation with GSIS in vivo and in vitro, our data highlight 27 miRNAs, and two biological processes – respectively involving 21 and 19 genes - some of them not previously described in the context of beta cell physiology, as potentially important contributors to the resolution of diabetes after bariatric surgery. The systemic and intracellular mechanisms through which surgery leads to these changes in the islet are likely to provide exciting questions for future research.

Declaration of Competing Interest

G.R. has received research grant funding from Sun Pharmaceuticals Inc and Les Laboratoires Servier, and is a consultant for Sun Pharmaceuticals. Other authors have nothing to disclose.

Acknowledgements

Authors thank physicians (Prof Christine Poitou and Dr Judith Aron-Wisnewsky) and clinical research staff (Dr Florence Marchelli) for patient recruitment, phenotyping and data management.

Funding

This project has received funding from the European Union's Horizon 2020 research and innovation programme via the Innovative Medicines Initiative 2 Joint Undertaking under grant agreement No 115881 (RHAPSODY) to G.A.R., C.M. and R.S. This Joint Undertaking receives support from the European Union's Horizon 2020 research and innovation programme and EFPIA. C.A. received grants for this work by INSERM (poste d'accueil INSERM), Société Francophone du Diabète and Institut Benjamin Delessert. G.A.R. was supported by a Wellcome Trust Investigator Award (212625/Z/18/Z), MRC Programme grants (MR/R022259/1, MR/J0003042/1, MR/L020149/1) and by Diabetes UK (BDA/11/0004210, BDA/15/0005275, BDA 16/0005485) project grants. RR was supported by National Science Foundation (310030−188447). F.A. received a grant by Fondation de l'Avenir for this work. Funders had no role in study design, data collection, data analysis, interpretation, writing of the report.

Supplementary materials

Supplementary material associated with this article can be found, in the online version, at doi:10.1016/j.ebiom.2020.102895.

References

[1] Andreelli F, Amouyal C, Magnan C, Mithieux G. What can bariatric surgery teach us about the pathophysiology of type 2 diabetes? Diabetes Metab 2009;35(6 Pt 2):499–507.
[2] Frühbeck G. Bariatric and metabolic surgery: a shift in eligibility and success criteria. Nat Rev Endocrinol 2015;11(8):465–77.

[3] Chambers AP, Jessen L, Ryan KK, Sisley S, Wilson−Pérez HE, Stefater MA, et al. Weight-independent changes in blood glucose homeostasis after gastric bypass or vertical sleeve gastrectomy in rats. Gastroenterology 2011;141(3):950–8.
[4] Cohen RV, Rubino F, Schiavon C, Cummings DE. Diabetes remission without weight loss after duodenal bypass surgery. Surg Obes Relat Dis Off J Am Soc Bariatr Surg 2012;8(5):e66–8.
[5] Pories WJ, Swanson MS, MacDonald KG, Long SB, Morris PG, Brown BM, et al. Who would have thought it? An operation proves to be the most effective therapy for adult-onset diabetes mellitus. Ann Surg 1995;222(3):339–50 discussion 350-352.
[6] Arble DM, Sandoval DA, Seeley RJ. Mechanisms underlying weight loss and metabolic improvements in rodent models of bariatric surgery. Diabetologia 2015;58(2):211–20.
[7] Evers SS, Sandoval DA, Seeley RJ. The physiology and molecular underpinnings of the effects of bariatric surgery on obesity and diabetes. Annu Rev Physiol 2017 10;79:313–34.
[8] Amouyal C, Andreelli F. Increasing GLP-1 circulating levels by bariatric surgery or by GLP-1 receptor agonists therapy: why are the clinical consequences so different? J Diabetes Res 2016;2016:1–10.
[9] Laferrère B. Diabetes remission after bariatric surgery: is it just the incretins? Int J Obes 2005 2011;35(Suppl 3):S22–5.
[10] Douros JD, Lewis AG, Smith EP, Niu J, Capozzi M, Wittmann A, et al. Enhanced glucose control following vertical sleeve gastrectomy does not require a β-Cell glucagon-like peptide 1 receptor. Diabetes 2018;67(8):1504–11.
[11] Mokadem M, Zechner JF, Margolskee RF, Drucker DJ, Aguirre V. Effects of Roux-en-Y gastric bypass on energy and glucose homeostasis are preserved in two mouse models of functional glucagon-like peptide-1 deficiency. Mol Metab 2014;3(2):191–201.
[12] Wilson-Pérez HE, Chambers AP, Ryan KK, Li B, Sandoval DA, Stoffers D, et al. Vertical sleeve gastrectomy is effective in two genetic mouse models of glucagon-like Peptide 1 receptor deficiency. Diabetes 2013;62(7):2380–5.
[13] Troy S, Soty M, Ribeiro L, Laval L, Migrenne S, Fioramonti X, et al. Intestinal gluconeogenesis is a key factor for early metabolic changes after gastric bypass but not after gastric lap-band in mice. Cell Metab 2008;8(3):201–11.
[14] Holter MM, Dutia R, Stano SM, Prigeon RL, Homel P, McGinty JJ, et al. Glucose metabolism after gastric banding and gastric bypass in individuals with Type 2 diabetes: weight loss effect. Diabetes Care 2017;40(1):7–15.
[15] Bojsen-Møller KN, Dirksen C, Jørgensen NB, Jacobsen SH, Hansen DL, Worm D, et al. Increased Hepatic Insulin Clearance After Roux-en-Y Gastric Bypass. J Clin Endocrinol Metab 2013;98(6):E1066–71.
[16] Salehi M, Gastaldelli A, D'Alessio DA. Beta-cell sensitivity to insulinotropic gut hormones is reduced after gastric bypass surgery. Gut 2019;68(10):1838–45.
[17] Shah A, Holter MM, Rimawi F, Mark V, Dutia R, McGinty J, et al. Insulin Clearance After Oral and Intravenous Glucose Following Gastric Bypass and Gastric Banding Weight Loss. Diabetes Care 2019 Feb;42(2):311–7.
[18] American Diabetes Association. 2. Classification and Diagnosis of Diabetes: *standards of Medical Care in Diabetes—2018*. Diabetes Care 2018;41(Supplement 1):S13–27.
[19] Buse JB, Caprio S, Cefalu WT, Ceriello A, Del Prato S, Inzucchi SE, et al. How do we define cure of diabetes? Diabetes Care 2009;32(11):2133–5.
[20] Cani PD, Knauf C, Iglesias MA, Drucker DJ, Delzenne NM, Burcelin R. Improvement of glucose tolerance and hepatic insulin sensitivity by oligofructose requires a functional glucagon-like peptide 1 receptor. Diabetes 2006;55 (5):1484–90.
[21] Knop FK, Vilsbøll T, Højberg PV, Larsen S, Madsbad S, Vølund A, et al. Reduced incretin effect in type 2 diabetes: cause or consequence of the diabetic state? Diabetes 2007;56(8):1951–9.
[22] Viollet B, Andreelli F, Jørgensen SB, Perrin C, Geloen A, Flamez D, et al. The AMP-activated protein kinase α2 catalytic subunit controls whole-body insulin sensitivity. J Clin Invest 2003;111(1):91–8.
[23] Vestergaard A, Blankestijn M, Stahl J, Pallesen E, Bang-Berthelsen C, Pociot F, et al. A systematic comparison of purification and normalization protocols for quantitative MicroRNA expressional profiling in insulin-producing cells. Int J Mol Sci 2016;17(6):896.
[24] Salem V, Silva LD, Suba K, Georgiadou E, Neda Mousavy Gharavy S, Akhtar N, et al. Leader β-cells coordinate Ca2+ dynamics across pancreatic islets in vivo. Nat Metab 2019;1(6):615–29.
[25] Robinson MD, McCarthy DJ, Smyth GK. edgeR: a Bioconductor package for differential expression analysis of digital gene expression data. Bioinformatics 2010;26(1):139–40.
[26] Wickham H. Ggplot2: elegant graphics for data analysis. New York: Springer; 2009. p. 212 p..
[27] Yu G, Wang L-G, Han Y, He Q-Y. clusterProfiler: an R package for comparing biological themes among gene clusters. OMICS J Integr Biol 2012 May;16(5): 284–7.
[28] Yu G, Li F, Qin Y, Bo X, Wu Y, Wang S. GOSemSim: an R package for measuring semantic similarity among GO terms and gene products. Bioinformatics 2010 Apr 1;26(7):976–8.
[29] Agarwal V, Bell GW, Nam J-W, Bartel DP. Predicting effective microRNA target sites in mammalian mRNAs. eLife [Internet]. [cited 2019 Apr 20];4. Available from: https://elifesciences.org/articles/05005.
[30] Shannon P. Cytoscape: a software environment for integrated models of biomolecular interaction networks. Genome Res 2003 Nov 1;13(11):2498–504.
[31] Surwit RS, Feinglos MN, Livingston EG, Kuhn CM, McCubbin JA. Behavioral manipulation of the diabetic phenotype in ob/ob mice. Diabetes 1984 Jul;33 (7):616–8.
[32] Carrasco F, Papapietro K, Csendes A, Salazar G, Echenique C, Lisboa C, et al. Changes in resting energy expenditure and body composition after weight loss following Roux-en-Y gastric bypass. Obes Surg 2007 May;17(5):608–16.
[33] Stefater MA, Pérez-Tilve D, Chambers AP, Wilson-Pérez HE, Sandoval DA, Berger J, et al. Sleeve gastrectomy induces loss of weight and fat mass in obese rats, but does not affect leptin sensitivity. Gastroenterology 2010;138(7):2426–36 2436. e1-3.
[34] Stefater MA, Wilson-Pérez HE, Chambers AP, Sandoval DA, Seeley RJ. All bariatric surgeries are not created equal: insights from mechanistic comparisons. Endocr Rev 2012;33(4):595–622.
[35] Stylopoulos N, Hoppin AG, Kaplan LM. Roux-en-Y gastric bypass enhances energy expenditure and extends lifespan in diet-induced obese rats. Obes Silver Spring Md 2009;17(10):1839–47.
[36] Wardé-Kamar J, Rogers M, Flancbaum L, Laferrère B. Calorie intake and meal patterns up to 4 years after Roux-en-Y gastric bypass surgery. Obes Surg 2004 Sep;14(8):1070–9.
[37] Rubino F, Nathan DM, Eckel RH, Schauer PR, Alberti KGMM, Zimmet PZ, et al. Metabolic surgery in the treatment algorithm for Type 2 diabetes: a joint statement by international diabetes organizations. Diabetes Care 2016 Jun 1;39 (6):861–77.
[38] Schauer PR, Bhatt DL, Kirwan JP, Wolski K, Aminian A, Brethauer SA, et al. Bariatric Surgery versus Intensive Medical Therapy for Diabetes - 5-Year Outcomes. N Engl J Med 2017 16;376(7):641–51.
[39] Baetens D, Stefan Y, Ravazzola M, Malaisse-Lagae F, Coleman DL, Orci L. Alteration of islet cell populations in spontaneously diabetic mice. Diabetes 1978;27 (1):1–7.
[40] Bock T, Pakkenberg B, Buschard K. Increased islet volume but unchanged islet number in ob/ob mice. Diabetes 2003;52(7):1716–22.
[41] Saleh MC. Endogenous islet uncoupling protein-2 expression and loss of glucose homeostasis in ob/ob mice. J Endocrinol 2006;190(3):659–67.
[42] Jetton TL, Liang Y, Cincotta AH. Systemic treatment with sympatholytic dopamine agonists improves aberrant beta-cell hyperplasia and GLUT2, glucokinase, and insulin immunoreactive levels in ob/ob mice. Metabolism 2001;50 (11):1377–84.
[43] Ishida E, Kim-Muller JY, Accili D. Pair feeding, but not insulin, phloridzin, or rosiglitazone treatment, curtails markers of β-cell dedifferentiation in *db/db* mice. Diabetes 2017;66(8):2092–101.
[44] Diedisheim M, Oshima M, Albagli O, Huldt CW, Ahlstedt I, Clausen M, et al. Modeling human pancreatic beta cell dedifferentiation. Mol Metab 2018;10:74–86.
[45] Pullen TJ, Sylow L, Sun G, Halestrap AP, Richter EA, Rutter GA. Overexpression of monocarboxylate transporter-1 (Slc16a1) in mouse pancreatic -cells leads to relative hyperinsulinism during exercise. Diabetes 2012;61(7):1719–25.
[46] Pullen TJ, Huising MO, Rutter GA. Analysis of purified pancreatic islet beta and alpha cell transcriptomes reveals 11β-Hydroxysteroid dehydrogenase (Hsd11b1) as a novel disallowed gene. Front Genet 2017 [Internet][cited 2020 Mar 10];08. Available from: http://journal.frontiersin.org/article/10.3389/fgene.2017.00041/full.
[47] Asghar A, Sheikh N. Role of immune cells in obesity induced low grade inflammation and insulin resistance. Cell Immunol 2017;315:18–26.
[48] Khodabandehloo H, Gorgani-Firuzjaee S, Panahi G, Meshkani R. Molecular and cellular mechanisms linking inflammation to insulin resistance and β-cell dysfunction. Transl Res J Lab Clin Med 2016;167(1):228–56.
[49] Chan JY, Luzuriaga J, Bensellam M, Biden TJ, Laybutt DR. Failure of the adaptive unfolded protein response in islets of obese mice is linked with abnormalities in β-cell gene expression and progression to diabetes. Diabetes 2013;62(5):1557–68.
[50] Eguchi K, Manabe I, Oishi-Tanaka Y, Ohsugi M, Kono N, Ogata F, et al. Saturated fatty acid and TLR signaling link β cell dysfunction and islet inflammation. Cell Metab 2012;15(4):518–33.
[51] Irles E, Ñeco P, Lluesma M, Villar-Pazos S, Santos-Silva JC, Vettorazzi JF, et al. Enhanced glucose-induced intracellular signaling promotes insulin hypersecretion: pancreatic beta-cell functional adaptations in a model of genetic obesity and prediabetes. Mol Cell Endocrinol 2015;404:46–55.
[52] Colsoul B, Jacobs G, Philippaert K, Owsianik G, Segal A, Nilius B, et al. Insulin downregulates the expression of the Ca2+-activated nonselective cation channel TRPM5 in pancreatic islets from leptin-deficient mouse models. Pflugers Arch 2014;466(3):611–21.
[53] Gonzalez A, Merino B, Marroquí L, Ñeco P, Alonso-Magdalena P, Caballero-Garrido E, et al. Insulin hypersecretion in islets from diet-induced hyperinsulinemic obese female mice is associated with several functional adaptations in individual β-Cells. Endocrinology 2013 Oct;154(10):3515–24.
[54] Ravier MA, Sehlin J, Henquin JC. Disorganization of cytoplasmic Ca(2+) oscillations and pulsatile insulin secretion in islets from ob/ obmice. Diabetologia 2002 Aug;45(8):1154–63.
[55] Guay C, Regazzi R. New emerging tasks for microRNAs in the control of β-cell activities. Biochim Biophys Acta BBA - Mol Cell Biol Lipids 2016 Dec;1861 (12):2121–9.
[56] LaPierre MP, Stoffel M. MicroRNAs as stress regulators in pancreatic beta cells and diabetes. Mol Metab 2017;6(9):1010–23.
[57] Martinez-Sanchez A, Rutter GA, Latreille M. MiRNAs in β-cell development, identity, and disease. Front Genet 2017 Jan 11 [Internet][cited 2020 Mar 11];7. Available from: http://journal.frontiersin.org/article/10.3389/fgene.2016.00226/full.
[58] Nesca V, Guay C, Jacovetti C, Menoud V, Peyot M-L, Laybutt DR, et al. Identification of particular groups of microRNAs that positively or negatively impact on beta cell function in obese models of type 2 diabetes. Diabetologia 2013;56 (10):2203–12.

[59] Rodríguez-Comas J, Moreno-Asso A, Moreno-Vedia J, Martín M, Castaño C, Marzà-Florensa A, et al. Stress-Induced MicroRNA-708 Impairs β-Cell Function and Growth. Diabetes 2017;66(12):3029–40.

[60] Tattikota SG, Rathjen T, McAnulty SJ, Wessels H-H, Akerman I, van de Bunt M, et al. Argonaute2 Mediates Compensatory Expansion of the Pancreatic β Cell. Cell Metab 2014;19(1):122–34.

[61] Zhao E, Keller MP, Rabaglia ME, Oler AT, Stapleton DS, Schueler KL, et al. Obesity and genetics regulate microRNAs in islets, liver, and adipose of diabetic mice. Mamm Genome 2009;20(8):476–85.

[62] Feng J, Xing W, Xie L. Regulatory Roles of MicroRNAs in Diabetes. Int J Mol Sci 2016;17(10):1729.

[63] Guay C, Regazzi R. Circulating microRNAs as novel biomarkers for diabetes mellitus. Nat Rev Endocrinol 2013;9(9):513–21.

[64] Keller A, Leidinger P, Bauer A, ElSharawy A, Haas J, Backes C, et al. Toward the blood-borne miRNome of human diseases. Nat Methods 2011;8(10):841–3.

[65] Debédat J, Sokolovska N, Coupaye M, Panunzi S, Chakaroun R, Genser L, et al. Long-term Relapse of Type 2 Diabetes After Roux-en-Y Gastric Bypass: prediction and Clinical Relevance. Diabetes Care 2018;41(10):2086–95.

[66] Douros JD, Tong J, D'Alessio DA. The Effects of Bariatric Surgery on Islet Function, Insulin Secretion, and Glucose Control. Endocr Rev 2019;40(5):1394–423.

[67] Gastaldelli A, Iaconelli A, Gaggini M, Magnone MC, Veneziani A, Rubino F, et al. Short-term Effects of Laparoscopic Adjustable Gastric Banding Versus Roux-en-Y Gastric Bypass. Diabetes Care 2016;39(11):1925–31.

[68] Mingrone G, Cummings DE. Changes of insulin sensitivity and secretion after bariatric/metabolic surgery. Surg Obes Relat Dis 2016;12(6):1199–205.

[69] Hao Z, Münzberg H, Rezai-Zadeh K, Keenan M, Coulon D, Lu H, et al. Leptin deficient ob/ob mice and diet-induced obese mice responded differently to Roux-en-Y bypass surgery. Int J Obes 2005 2015;39(5):798–805.

[70] Mokadem M, Zechner JF, Uchida A, Aguirre V. Leptin is required for glucose homeostasis after Roux-en-Y gastric bypass in mice. Claret M, editor. Leptin is required for glucose homeostasis after Roux-en-Y gastric bypass in mice. PLoS ONE 2015 Oct 7;10(10):e0139960.

[71] Douros JD, Niu J, Sdao S, Gregg T, Merrins MJ, Campbell J, et al. Temporal plasticity of insulin and incretin secretion and insulin sensitivity following sleeve gastrectomy contribute to sustained improvements in glucose control. Mol Metab 2019;28:144–50.

[72] Kim-Muller JY, Fan J, Kim YJR, Lee S-A, Ishida E, Blaner WS, et al. Aldehyde dehydrogenase 1a3 defines a subset of failing pancreatic β cells in diabetic mice. Nat Commun 2016 Nov [Internet][cited 2020 Jan 24];7(1). Available from: http://www.nature.com/articles/ncomms12631.

[73] Seyfried F, Miras AD, Rotzinger L, Nordbeck A, Corteville C, Li JV, et al. Gastric bypass-related effects on glucose control, β cell function and morphology in the obese Zucker Rat. Obes Surg 2016;26(6):1228–36.

[74] Sun X, Zheng M, Song M, Bai R, Cheng S, Xing Y, et al. Ileal interposition reduces blood glucose levels and decreases insulin resistance in a type 2 diabetes mellitus animal model by up-regulating glucagon-like peptide-1 and its receptor. Int J Clin Exp Pathol 2014;7(7):4136–42.

[75] Salehi M, Prigeon RL, D'Alessio DA. Gastric bypass surgery enhances glucagon-like peptide 1-stimulated postprandial insulin secretion in humans. Diabetes 2011 Sep;60(9):2308–14.

[76] Nicolaus M, Brödl J, Linke R, Woerle H-J, Göke B, Schirra J. Endogenous GLP-1 Regulates Postprandial Glycemia in Humans: relative Contributions of Insulin, Glucagon, and Gastric Emptying. J Clin Endocrinol Metab 2011;96(1):229–36.

[77] Schirra J, Nicolaus M, Woerle HJ, Struckmeier C, Katschinski M, Göke B. GLP-1 regulates gastroduodenal motility involving cholinergic pathways. Neurogastroenterol Motil 2009 Jun;21(6):609–e22.

[78] Douros JD, Niu J, Sdao SM, Gregg T, Fisher-Wellman KH, Bharadwaj MS, et al. Sleeve gastrectomy rapidly enhances islet function independently of body weight. JCI Insight 2019 Feb 19 [Internet][cited 2019 Apr 4]; Available from: http://insight.jci.org/articles/view/126688.

[79] Zhang CY, Baffy G, Perret P, Krauss S, Peroni O, Grujic D, et al. Uncoupling protein-2 negatively regulates insulin secretion and is a major link between obesity, beta cell dysfunction, and type 2 diabetes. Cell 2001 Jun 15;105(6):745–55.

[80] Bleisch VR, Mayer J, Dickie MM. Familial diabetes mellitus in mice, associated with insulin resistance, obesity, and hyperplasia of the islands of langerhans. Am J Pathol 1952 Jun;28(3):369–85.

[81] Starich GH, Zafirova M, Jablenska R, Petkov P, Lardinois CK. A morphological and immunohistochemical investigation of endocrine pancreata from obese ob+/ob+ mice. Acta Histochem 1991 Jan;90(1):93–101.

[82] Rutter GA, Pullen TJ, Hodson DJ, Martinez-Sanchez A. Pancreatic β-cell identity, glucose sensing and the control of insulin secretion. Biochem J 2015 Mar 1;466(2):203–18.

[83] Matschinsky FM, Wilson DF. The central role of glucokinase in glucose homeostasis: a perspective 50 years after demonstrating the presence of the enzyme in islets of langerhans. Front Physiol 2019;10:148.

[84] Doliba NM, Qin W, Najafi H, Liu C, Buettger CW, Sotiris J, et al. Glucokinase activation repairs defective bioenergetics of islets of Langerhans isolated from type 2 diabetics. Am J Physiol Endocrinol Metab 2012 Jan 1;302(1):E87–102.

[85] Osbak KK, Colclough K, Saint-Martin C, Beer NL, Bellanné-Chantelot C, Ellard S, et al. Update on mutations in glucokinase (GCK), which cause maturity-onset diabetes of the young, permanent neonatal diabetes, and hyperinsulinemic hypoglycemia. Hum Mutat 2009 Nov;30(11):1512–26.

[86] Arden C, Hampson LJ, Huang GC, Shaw JAM, Aldibbiat A, Holliman G, et al. A role for PFK-2/FBPase-2, as distinct from fructose 2,6-bisphosphate, in regulation of insulin secretion in pancreatic beta-cells. Biochem J 2008 Apr 1;411(1):41–51.

[87] Gerst F, Jaghutriz BA, Staiger H, Schulte AM, Lorza-Gil E, Kaiser G, et al. The Expression of Aldolase B in Islets Is Negatively Associated With Insulin Secretion in Humans. J Clin Endocrinol Metab 2018 Dec 1;103(12):4373–83.

[88] Ni Q, Gu Y, Xie Y, Yin Q, Zhang H, Nie A, et al. Raptor regulates functional maturation of murine beta cells. Nat Commun 2017;8:15755. 09.

[89] Esguerra JLS, Nagao M, Ofori JK, Wendt A, Eliasson L. MicroRNAs in islet hormone secretion. Diabetes Obes Metab 2018;20(Suppl 2):11–9.

[90] He Y, Ding Y, Liang B, Lin J, Kim T-K, Yu H, et al. A Systematic Study of Dysregulated MicroRNA in Type 2 Diabetes Mellitus. Int J Mol Sci 2017 Feb 28;18(3):456.

[91] Liang YZ, Li JJ, Xiao HB, He Y, Zhang L, Yan YX. YX. Identification of stress-related microRNA biomarkers in type 2 diabetes mellitus: A systematic review and meta-analysis [published online ahead of print, 2018 Jan 17]. J Diabetes 2018. doi: 10.1111/1753-0407.12643.

[92] Roat R, Hossain MM, Christopherson J, Free C, Jain S, Guay C, et al. Identification and characterization of microRNAs associated with human β-Cell loss in a mouse model. Am J Transplant Off J Am Soc Transplant Am Soc Transpl Surg 2017;17(4):992–1007.

[93] Ofori JK, Salunkhe VA, Bagge A, Vishnu N, Nagao M, Mulder H, et al. Elevated miR-130a/miR130b/miR-152 expression reduces intracellular ATP levels in the pancreatic beta cell. Sci Rep 2017 Dec [Internet][cited 2019 Mar 14];7(1). Available from: http://www.nature.com/articles/srep44986.

[94] Tsukita S, Yamada T, Takahashi K, Munakata Y, Hosaka S, Takahashi H, et al. MicroRNAs 106b and 222 improve hyperglycemia in a mouse model of insulin-deficient diabetes via pancreatic β-Cell proliferation. EBioMedicine 2017 Feb;15:163–72.

[95] Zheng Y, Wang Z, Tu Y, Shen H, Dai Z, Lin J, et al. miR-101a and miR-30b contribute to inflammatory cytokine-mediated β-cell dysfunction. Lab Invest 2015 Dec;95(12):1387–97.

[96] Alkandari A, Ashrafian H, Sathyapalan T, Sedman P, Darzi A, Holmes E, et al. Improved physiology and metabolic flux after Roux-en-Y gastric bypass is associated with temporal changes in the circulating microRNAome: a longitudinal study in humans. BMC Obes 2018 Dec [Internet][cited 2019 Mar 15];5(1). Available from: https://bmcobes.biomedcentral.com/articles/10.1186/s40608-018-0199-z.

[97] Bae Y-U, Kim Y, Lee H, Kim H, Jeon JS, Noh H, et al. Bariatric surgery alters microRNA content of circulating exosomes in patients with obesity: exosomal miRNA profiling in patients with obesity. Obesity 2019 Feb;27(2):264–71.

[98] Hubal MJ, Nadler EP, Ferrante SC, Barberio MD, Suh J-H, Wang J, et al. Circulating adipocyte-derived exosomal MicroRNAs associated with decreased insulin resistance after gastric bypass: gastric Bypass Alters Exosomal MicroRNAs. Obesity 2017;25(1):102–10.

[99] Nunez Lopez YO, Coen PM, Goodpaster BH, Seyhan AA. Gastric bypass surgery with exercise alters plasma microRNAs that predict improvements in cardiometabolic risk. Int J Obes 2017;41(7):1121–30.

[100] Atkin SL, Ramachandran V, Yousri NA, Benurwar M, Simper SC, McKinlay R, et al. Changes in Blood microRNA Expression and Early Metabolic Responsiveness 21 Days Following Bariatric Surgery. Front Endocrinol 2019 Jan 4 [Internet][cited 2019 Mar 15];9. Available from: https://www.frontiersin.org/article/10.3389/fendo.2018.00773/full.

[101] Lirun K, Sewe M, Yong W. A pilot study: the effect of Roux-en-Y gastric bypass on the serum MicroRNAs of the Type 2 diabetes patient. Obes Surg 2015 Dec;25(12):2386–92.

[102] Zhu Z, Yin J, Li DC, Mao ZQ. Role of microRNAs in the treatment of type 2 diabetes mellitus with Roux-en-Y gastric bypass. Braz J Med Biol Res 2017;50(3) [Internet][cited 2019 Mar 15]Available from: http://www.scielo.br/scielo.php?script=sci_arttext&pid=S0100-879X2017000300705&lng=en&tlng=en.

[103] Hofsø D, Fatima F, Borgeraas H, Birkeland KI, Gulseth HL, Hertel JK, et al. Gastric bypass versus sleeve gastrectomy in patients with type 2 diabetes (Oseberg): a single-centre, triple-blind, randomised controlled trial. Lancet Diabetes Endocrinol 2019 Dec;7(12):912–24.

[104] Galtier F, Pattou F, Czernichow S, Disse E, Ritz P, Chevallier J-M, et al. Bariatric surgery and the perioperative management of type 2 diabetes: practical guidelines. J Visc Surg 2020 Feb;157(1):13–21.

[105] Hatoum IJ, Stylopoulos N, Vanhoose AM, Boyd KL, Yin DP, Ellacott KLJ, et al. Melanocortin-4 Receptor Signaling Is Required for Weight Loss after Gastric Bypass Surgery. J Clin Endocrinol Metab 2012 Jun;97(6):E1023–31.